1521-0111/90/3/162–176$25.00
MOLECULAR PHARMACOLOGY

http://dx.doi.org/10.1124/mol.116.104505
Mol Pharmacol 90:162–176, September 2016

Quantitative Single-Cell Analysis of Signaling Pathways Activated Immediately Downstream of Histamine Receptor Subtypes[S]

Jakobus van Unen, Ali Rashidfarrokhi,[1] Eelco Hoogendoorn, Marten Postma, Theodorus W. J. Gadella, Jr., and Joachim Goedhart

Swammerdam Institute for Life Sciences, Section of Molecular Cytology, van Leeuwenhoek Centre for Advanced Microscopy, University of Amsterdam, Amsterdam, The Netherlands

Received March 31, 2016; accepted June 28, 2016

ABSTRACT

Genetically encoded biosensors based on Förster resonance energy transfer (FRET) can visualize responses of individual cells in real time. Here, we evaluated whether FRET-based biosensors provide sufficient contrast and specificity to measure activity of G-protein–coupled receptors. The four histamine receptor subtypes (H_1R, H_2R, H_3R, and H_4R) respond to the ligand histamine by activating three canonical heterotrimeric G-protein–mediated signaling pathways with a reported high degree of specificity. Using FRET-based biosensors, we demonstrate that H_1R activates Gαq. We also observed that H_1R activates Gαi, albeit at a 10-fold lower potency. In addition to increasing cAMP levels, most likely via Gαs, we found that the H_2R induces Gαq-mediated calcium release. The H_3R and H_4R activated Gαi with high specificity and a high potency. We demonstrate that a number of FRET sensors provide sufficient contrast to: 1) analyze the specificity of the histamine receptor subtypes for different heterotrimeric G-protein families with single-cell resolution, 2) probe for antagonist specificity, and 3) allow the measurement of single-cell concentration-response curves.

Introduction

The histamine receptor family consists of four known members to date: histamine-1-receptor (H_1R), histamine-2-receptor (H_2R), histamine-3-receptor (H_3R), and the more recently discovered histamine-4-receptor (H_4R) (Jablonowski et al., 2004). Although the sequence homology is relatively low (e.g., H_4R shares approximately 37% identity with the H_3R, but less than 20% with the H_2R and H_1R; Liu et al., 2001; Zhu et al., 2001), all subtypes bind histamine specifically. The histamine receptor family has been implicated in a large number of pathologies (Parsons and Ganellin, 2006; Pino-Ángeles et al., 2012), including cancer (Medina and Rivera, 2010), and is therefore a popular target for therapeutic interventions (Bongers et al., 2010; Seifert et al., 2013).

The H_1R is mainly expressed in endothelium, smooth muscle cells, and the central nervous system (CNS) and is best known for its role in various allergic disorders, such as hay fever, urticaria, and allergic rhinitis. The H_2R is ubiquitously expressed and its antagonists are widely used for the treatment of gastric ulcers. The H_3R is predominantly expressed in the CNS, and its antagonists are currently under investigation for the treatment of a wide range of CNS pathologies, including cognitive disorders, sleep disorders, and aberrant energy homeostasis. The H_4R is expressed in leukocytes and mast cells, and is thus possibly involved in inflammatory and immune responses (Thurmond et al., 2008).

Histamine receptors are G-protein–coupled receptors (GPCRs), and the different subtypes couple to distinct heterotrimeric G-protein families. Signaling downstream of the heterotrimeric G-protein complex is often attributed and classified according to the Gα subunit, since it defines the specific downstream signaling events that are activated. GPCRs can signal via four different Gα-protein families: Gαq, Gα12, Gαi, and Gαs (Fig. 1A). Furthermore, the accompanying G$\beta\gamma$ subunit also contributes to relaying the signal (Smrcka, 2008). In addition, signals are transduced via noncanonical pathways that involve β-arrestins (Ostermaier et al., 2014).

The signaling events directly downstream of the GPCR are used in cell-based screens aimed at identifying drugs that target GPCRs. Classically, Ca^{2+} and cAMP have been the second messengers of choice to detect GPCR activation.

Recently, new cell-based screens that measure alternative parameters and enable high-throughput analysis have been reported (Schröder et al., 2010; Inoue et al., 2012; Kroeze et al., 2015). The detection of Ca^{2+} is performed with Ca^{2+}-sensitive fluorescent probes, enabling real-time analysis. Since Gαq-mediated signaling efficiently activates Ca^{2+} release via

Part of this work is supported by NanoNextNL, a micro- and nanotechnology consortium of the Government of The Netherlands and 130 partners.
[1]Current affiliation: Department of Medicine, Langone Medical Center, New York University, New York.
dx.doi.org/10.1124/mol.116.104505.
[S] This article has supplemental material available at molpharm.aspetjournals.org.

ABBREVIATIONS: CFP, cyan fluorescent protein; CI, confidence interval; CNS, central nervous system; DORA, Dimerization Optimized Reporter for Activation; FRET, Förster resonance energy transfer; GPCR, G-protein–coupled receptor; HEK, human embryonic kidney 293; H_1R, histamine-1-receptor; H_2R, histamine-2-receptor; H_3R, histamine-3-receptor; H_4R, histamine-4-receptor; PCR, polymerase chain reaction; PLCβ, phospholipase C-β; PTX, pertussis toxin; RFP, red fluorescent protein; YFP, yellow fluorescent protein.

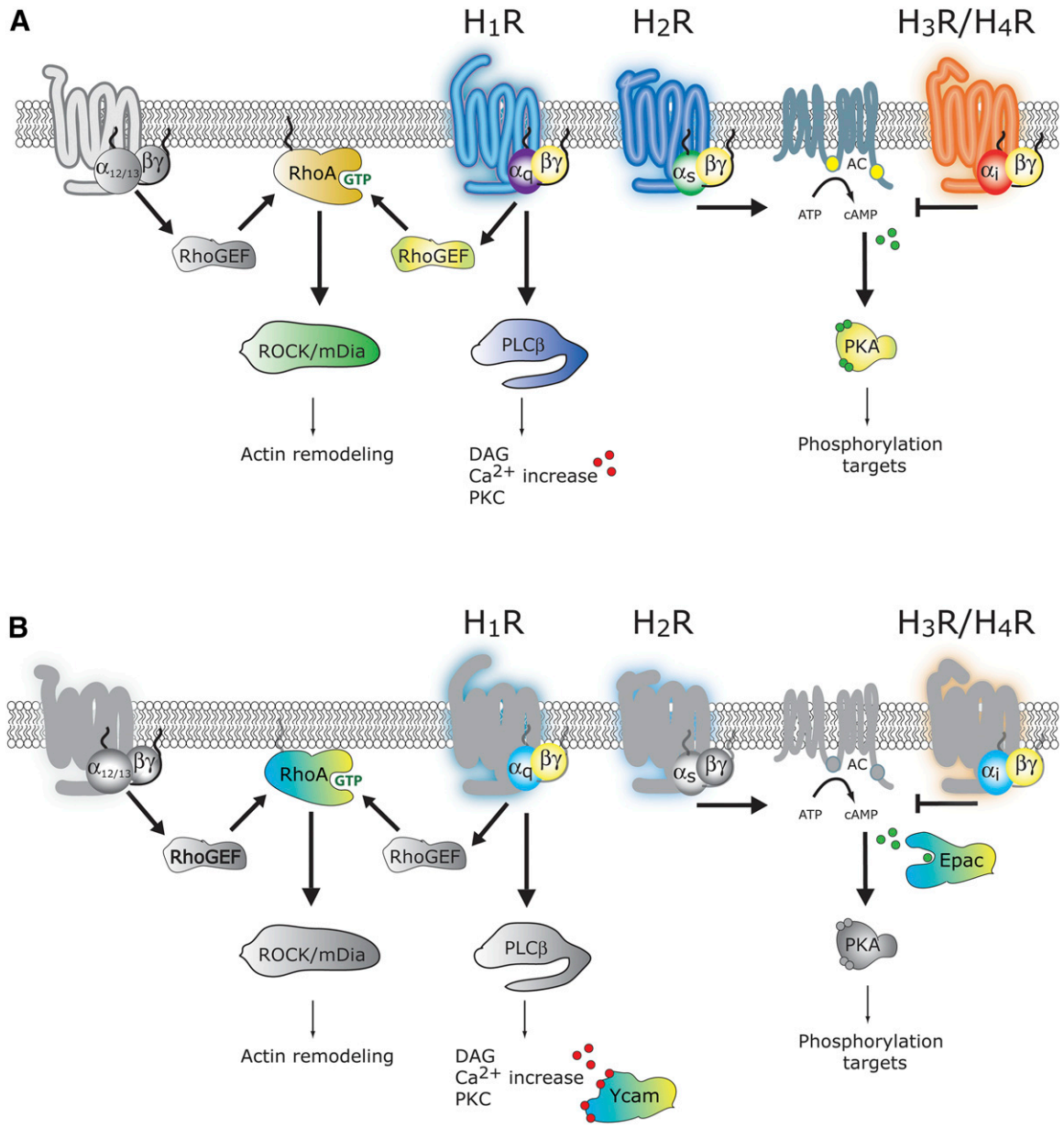

Fig. 1. Histamine receptor signaling. (A) Schematic overview of the canonical heterotrimeric G-protein–mediated signaling pathways activated by the four histamine receptor subtypes. (B) Overview of the different FRET biosensors used in this study to analyze the signaling profiles of the four histamine receptor subtypes. All biosensors are based on a CFP/YFP FRET pair. AC, adenylyl cyclase; DAG, diacylglycerol; mDia, mammalian diaphanous-related formin 1; PKA, protein kinase A; PKC, protein kinase C; RhoGEF, Rho guanine exchange factor; ROCK, Rho-associated coiled-coil-containing protein kinase.

phospholipase C-β (PLCβ), quantification of calcium levels is an important method to screen GPCR activity. To convert the activity of GPCRs that do not increase calcium levels, promiscuous G-proteins can be used (e.g., Gα_{16}) (Thomsen et al., 2005). Although calcium is a very sensitive readout due to magnification of the signal, Ca^{2+} is multiple steps downstream from the G-protein and influenced by cross-talk and signal amplification.

The cAMP levels are used to detect Gαs and Gαi signaling. However, the detection of Gαi activity often requires artificial elevation of cAMP levels by forskolin (Sensken et al., 2008). The detection of cAMP in general and Gαi activity in particular has limited temporal resolution. All of the high-content screening methods use population averages, and thus information on cell-to-cell heterogeneity is usually lost. Moreover, since single-cell resolution is not achieved, the strategies for detection of GPCR activation cannot report on spatial information of signaling events. The only exception is detection of Ca^{2+} with calcium-sensitive fluorophores.

Resonance energy transfer techniques have several unique properties that possibly allow new insights into GPCR signaling and their pharmacology, both in vitro and in vivo (Lohse et al., 2012; Clister et al., 2015; van Unen et al., 2015b). These techniques can provide quantitative data, on/off kinetics with high temporal resolution, can be measured in real time, and allow fast and straightforward analysis of the data (Marullo and Bouvier, 2007; Lohse et al., 2008). Specifically, genetically encoded Förster resonance energy transfer (FRET) sensors allow the assessment of cell-to-cell heterogeneity and the acquisition of multiple responses

from the same single cell in real time (Lohse et al., 2012). FRET reporters can be developed to measure every step in the GPCR signaling cascade. FRET biosensors are available to measure ligand binding to the GPCR (Stoddart et al., 2015), GPCR activation (Vilardaga et al., 2003), GPCR and G-protein interaction (Hein et al., 2005; Stumpf and Hoffmann, 2016), G-protein activation (Janetopoulos et al., 2001; Adjobo-Hermans et al., 2011), Ca^{2+} release (Nagai et al., 2004), cAMP production (Klarenbeek et al., 2015), and activation of downstream effectors such as protein kinase C (Verbeek et al., 2008), RhoA (van Unen et al., 2015a), and inositol 1,4,5-trisphosphate (Gulyás et al., 2015). The preferred option is to use FRET biosensors that report on the specific activation of one of the heterotrimeric G-protein subfamilies directly stimulated by a GPCR. Since this kind of biosensor is not yet available for all subclasses of G-proteins, we also made use of FRET biosensors that report on G-protein–mediated second-messenger production or activation. With the use of these biosensors, we characterized the canonical G-protein–mediated signaling profiles of the four histamine receptor subtypes. Moreover, we show that these techniques can be used to characterize ligand specificity and calculate potency at these receptors.

Materials and Methods

Construction of Fluorescent Protein Fusions. To obtain N1-xp2A-mCherry, two oligonucleotides encoding for the p2A viral peptide sequence ATNFSLLKQAGDVEENPGP (Kim et al., 2011) were annealed as previously described (Goedhart and Gadella, 2005). Annealing forward 5′-CCGGtggctactaacttcagcctgctgaagcaggctggagacgtggaggagaaccctggacctgggtc-3′ and reverse 5′-CATGgacccaggtccaggttctcctccacgtctccagcctgcttcagcaggctgaagttagtagcca-3′ oligonucleotides yielded the viral peptide xp2A sequence with overhangs (in capitals) on both sides, compatible with Age1 and Nco1 restriction sites. The double-stranded linker was ligated into an RSET-mCherry plasmid cut with AgeI and NcoI, resulting in RSET-xp2A-mCherry. This RSET-xp2A-mCherry plasmid was cut with Age1 and Bsrg1 and ligated into an empty clontech-style N1 vector, resulting in N1-xp2A-mCherry.

It turned out that this xP2A sequence was too short for efficient separation by the viral peptide sequence. To this end, three additional amino acids, GSG, were added to yield GSGATNFSLLKQAGDVEENPGP.

To add the GSG sequence, a PCR was performed on N1-xp2A-mCherry with forward primer 5′-TCCACCGGTGGGATCGGGTGCTACTAACTTCAGCCTGC-3′ and reverse primer 5′-TCTACAAATGTGGTATGGC-3′. The resulting pcr product was ligated into an empty clontech-style N1 vector using Age1 and Bsrg1 to create N1-p2A-mCherry.

Human histamine receptors were tagged with fluorescent proteins as described later. N1-H_1R-mCherry was obtained by cutting N1-mCherry with Nhe1 and Age1 and ligation with N1-H_1R-mTurquoise cut with the same enzymes. N1-H_1R-p2A-mCherry was made by cutting N1-p2A-mCherry with Age1 and Not1 and ligation with N1-H_1R-mCherry cut with the same enzymes. pcDNA3.1-H_2R (cDNA.org) was amplified using forward primer 5′-AGGTCTATATAAGCAGAGC-3′ and reverse primer 5′-AACCGCGGCCTGTCTGTGGCTCCCTG-3′. The pcr product was cut with HindIII and SacII and ligated into an N1-mCherry vector that was cut with the same enzymes. N1-H_2R-p2A-mCherry was made by cutting N1-p2A-mCherry with SacII and Bsrg1 and ligation with N1-H_2R-mCherry cut with the same enzymes.

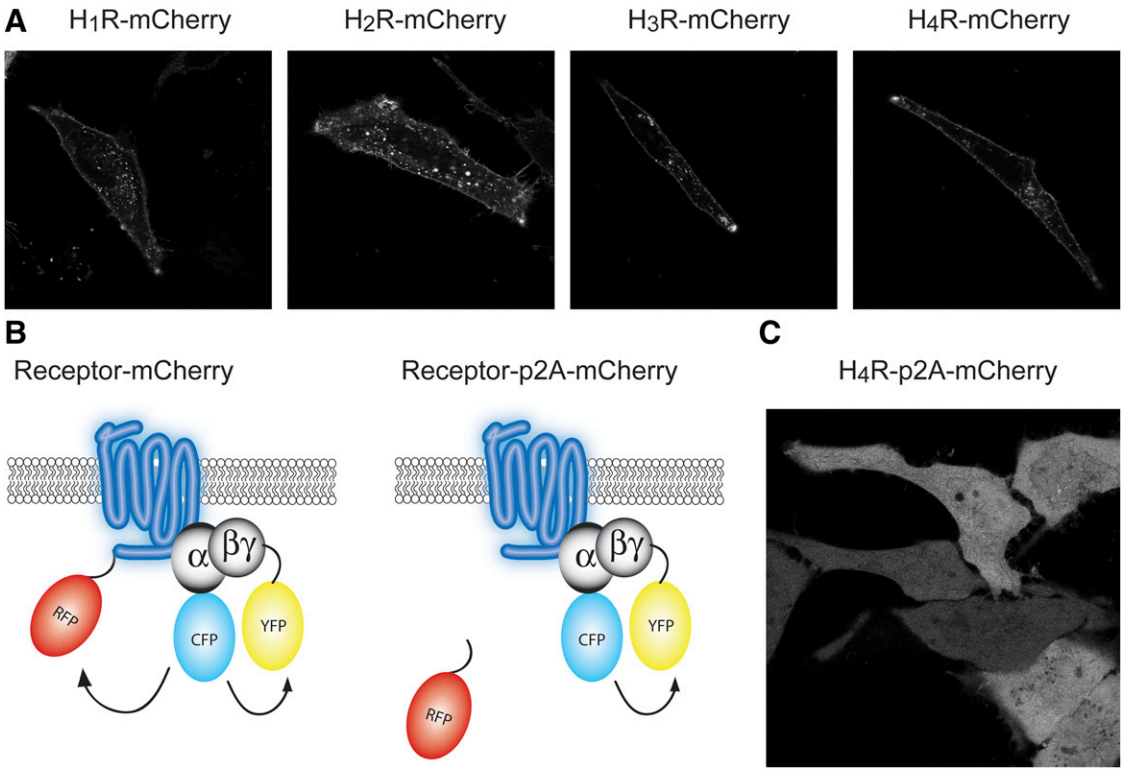

Fig. 2. Tagging histamine receptors with fluorescent proteins. (A) Representative confocal images of the localization of the four histamine receptor subtypes. HeLa cells were transiently transfected with a plasmid containing the indicated histamine receptor subtype directly fused to mCherry. (B) Schematic overview of the p2A tagging strategy. To prevent possible FRET between the CFP of a plasma membrane–localized biosensor and the RFP fused to the receptor (left), we introduced a p2A sequence between the receptor and the RFP, leading to separate expression of the RFP and receptor proteins. (C) Confocal image of HeLa cells transfected with the histamine-4-receptor fused to p2A-mCherry, showing the clear cytoplasmic localization of mCherry. Width of the individual images in (A) corresponds to 105 μm, and the width of the image in (C) corresponds to 117 μm.

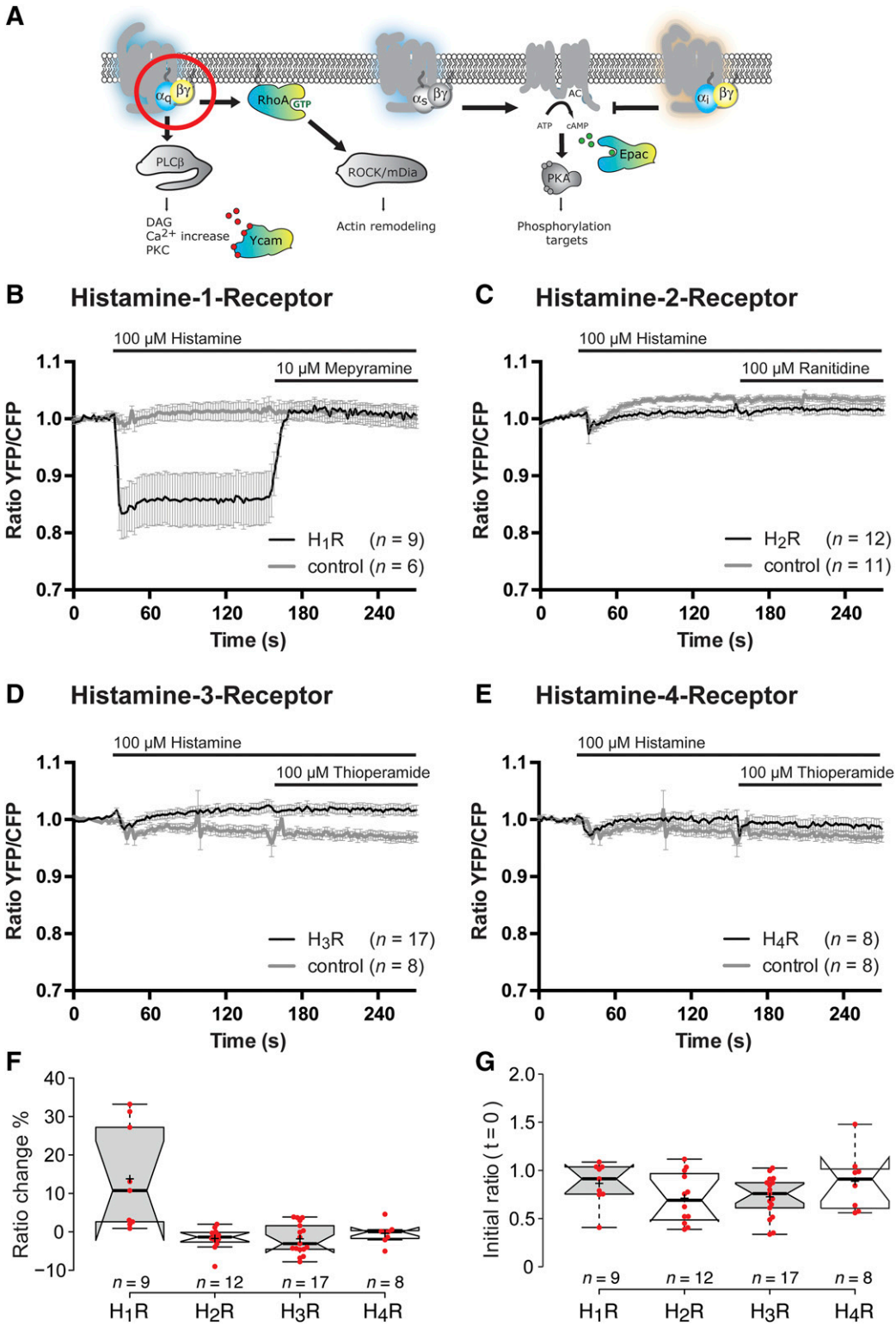

Fig. 3. Gαq signaling by histamine receptors. (A) Activation of the heterotrimeric G-protein Gαq by the four histamine receptor subtypes as measured by FRET ratio imaging. (B) Hela cells transfected with H_1R-p2A-RFP and the Gαq biosensor were treated with histamine and mepyramine (black). Control cells were transfected with only the Gαq biosensor (gray). (C) Cells transfected with H_2R-p2A-RFP and the Gαq biosensor were treated with histamine and ranitidine (black). In the control condition, cells were transfected only with the Gαq biosensor (gray). (D) Cells transfected with H_3R-p2A-RFP and the Gαq biosensor were treated with histamine and thioperamide (black). In the control condition, cells were transfected with only the Gαq biosensor (gray). (E) Cells transfected with H_4R-p2A-RFP and the Gαq biosensor were treated with histamine and thioperamide (black). In the control condition, cells were only transfected with the Gαq (gray). The median and average (+) amplitude of the FRET ratio change at t = 100 seconds (F) and the raw YFP/CFP ratio at t = 0 seconds (G) per receptor subtype, quantified from the experiments shown in (B–E). Box limits indicate the 25th and 75th percentiles as determined by R software (http://www.r-project.org); whiskers extend 1.5 times the interquartile range from the 25th and 75th percentiles. HeLa cells were stimulated with histamine at t = 32 seconds, and the response was antagonized by the addition of the appropriate antagonist at t = 152 seconds. Time traces show the average ratio change of YFP/CFP fluorescence (± S.E.M.). AC, adenylyl cyclase; DAG, diacylglycerol; mDia, mammalian diaphanous-related formin 1; PKA, protein kinase A; PKC, protein kinase C; ROCK, XXX.

pcDNA3.1-H_3R (cDNA.org) was amplified using forward primer 5′-AGGTCTATATAAGCAGAGC-3′ and reverse primer 5′-ATACCGGTCCCTTCCAGCAGTGCTCCAG-3′. The pcr product was cut with HindIII and Age1 and ligated into an N1-mCherry vector that was cut with the same enzymes. N1-H_3R-p2A-mCherry was made by cutting N1-p2A-mCherry with Age1 and Bsrg1 and ligation with N1-H_3R-mCherry cut with the same enzymes.

pDEF-H_4R-mVenus (a kind gift from Henry Vischer, Vrije University, Amsterdam, The Netherlands) was amplified with reverse primer ATaccggtGTAGAAGATACTGACCGACTG and forward primer CAGGTGTCGTGAGGAATTAG, and the product was cut with Age1 and Acc561. This product was ligated into an N1-mTurquoise2 vector that was also cut with Age1 and Acc561, resulting in N1-H_4R-mTurquoise2. mTurquoise2 was swapped for mCherry and p2A-mCherry by cutting N1-mCherry and N1-p2A-mCherry with Age1 and Not1 and ligation with N1-H_4R-mTurquoise2 cut with the same enzymes, resulting in N1-H_4R-mCherry and N1-H_4R-p2A-mCherry. The histamine receptors are available from Addgene.org.

A plasmid encoding YCam3.6 (Ycam, Middlesex, UK) was described previously (van Unen et al., 2015a). ^{T}EPAC^{VV} was as previously described (Klarenbeek et al., 2011). The dimerization optimized reporter for activation (DORA) RhoA sensor was a kind gift from Yi Wu and Taofei Yin (van Unen et al., 2015a) (University of Connecticut Health Center, Farmington, CT). The FRET biosensors for Gαq activation (Adjobo-Hermans et al., 2011) and Gαi activation (van Unen et al., 2016) were previously described.

Drug Treatments. The different histamine receptors were stimulated at the indicated time points as follows, unless otherwise specified. All substances were purchased from Sigma-Aldrich (Zwijndrecht, The Netherlands), except FR900359 and methylhistaprodifen. FR900359 was purchased from the University of Bonn (Bonn, Germany). Methylhistaprodifen (Elz et al., 2000) was a kind gift from Andrea Strasser and Sigurd Elz (Universität Regensburg, Regensburg, Germany). Drugs were dissolved in H_2O as 1000× concentrated stock solutions. Methylhistaprodifen was dissolved in dimethylsulfoxide at 100 and 10 mM and lower concentrations in dimethylsulfoxide/H_2O 1:1 (v/v). One microliter of the drug was added to a cell chamber containing 1 ml of liquid followed by rapid mixing by repeated pipetting of the medium. H_1R was stimulated with 100 μM histamine and deactivated by 10 μM mepyramine. H_2R was stimulated with 100 μM histamine and deactivated by 100 μM ranitidine. The H_3R and H_4R were stimulated with 100 μM histamine and deactivated by 100 μM thioperamide.

For Fig. 5, all receptors were stimulated with 100 μM histamine and 100 μM carbachol. Where indicated, cells were incubated with 100 ng/ml pertussis toxin (PTX) overnight or for 2 hours with the Gαq inhibitor FR900359 (previously known as UBO-QIC) (Schrage et al., 2015) at a concentration of 2 μM.

Cell Culture and Sample Preparation. Cell culture, transfection, and live cell microscopy conditions were performed as previously described (van Unen et al., 2015a).

Widefield Microscopy. Ratiometric FRET measurements were performed using a previously described widefield fluorescence microscope (van Unen et al., 2015a). Typical exposure times ranged from 50–200 ms, and camera binning was set to 4 × 4. The 420-nm (slit width 30 nm) excitation light was reflected onto the sample by a 455DCLP dichroic mirror (Omega, Brattleboro, VT), and cyan fluorescent protein (CFP) emission was detected with a BP470/30 filter (Omega), and yellow fluorescent protein (YFP) emission was detected with a BP535/30 filter by rotating the filter wheel. Acquisitions were corrected for background signal and, for FRET ratio imaging, bleedthrough of CFP emission in the YFP channel (55% of the intensity measured in the CFP channel).

Image Analysis. ImageJ (National Institutes of Health, Bethesda, MD) was used to analyze the raw microscopy images. A custom script in Python (Python.org) was used to perform background subtractions, bleedthrough correction, and calculation of the normalized ratio per time point for individual cells. The output of Python was written to Excel (Microsoft, Redmond, WA). Graphs and statistics were conducted using GraphPad version 6.0 for Mac (GraphPad Software, La Jolla, CA; www.graphpad.com). The fit of the concentration-response curves was performed in GraphPad with the following equation: ratio = $\min_{ratio}$ + ($\max_{ratio}$ − $\min_{ratio}$)/(1 + 10^((−pEC_{50} − X)*n)), where $\min_{ratio}$ and $\max_{ratio}$ represent the experimentally obtained minimal and maximal ratio, respectively; X is the log of the histamine concentration; n represents the Hill coefficient; and pEC_{50} is the −log of the concentration (EC_{50}) at which 50% of the maximal effect is observed.

Confocal Microscopy. HeLa cells transfected with the indicated constructs were imaged using a Nikon A1 confocal microscope equipped with a 60× oil immersion objective (Plan Apochromat VC, NA 1.4; Nikon Instruments, Melville, NY). The pinhole size was set to 1 Airy unit (<0.8 μm). Samples were excited with a 561-nm laser line and reflected onto the sample by a 457/514/561 dichroic mirror. Red fluorescent protein (RFP) emission was filtered through a BP595/50 emission filter. Acquisitions were corrected for background signal.

Results

Overview of Histamine Receptor Signaling Pathways and Relevant FRET Sensors. To study the activation of processes immediately downstream of the four histamine receptor subtypes, we used several FRET biosensors (Fig. 1B). Since the H_1R, H_2R, and H_3R/H_4R activate well described, presumably specific classes of G-proteins, we used FRET biosensors that report on these pathways.

The H_1R is well known to couple to Gαq; therefore, we used an intermolecular FRET biosensor that directly measures the activation (e.g., GDP for GTP exchange) of the heterotrimeric G-protein Gαq by monitoring the separation of the Gα subunit and the Gγ subunit (Adjobo-Hermans et al., 2011). Furthermore, we used Ycam (Ycam), a unimolecular FRET sensor based on the Ca^{2+}-binding domains of calmodulin (Nagai et al., 2004), which measures changes in intracellular Ca^{2+} concentration upon Gαq-mediated activation of the PLCβ family. More recently, Gαq has been linked to the activation of RhoA via direct interaction with Rho guanine exchange factors (Lutz et al., 2007). To measure the activation of RhoA, we used the DORA RhoA biosensor. This unimolecular FRET sensor measures the GTP loading of RhoA via binding of the Rho-binding domain of PKN1 to the RhoA moiety on the sensor (van Unen et al., 2015a). It should be noted that this sensor might also report on the activity of Gα12/Gα13. The H_2R is best known to couple to the Gαs subfamily of G-proteins, which are known to stimulate the production of cAMP. There is a FRET biosensor available for the direct measurement of Gαs activation (Hein et al., 2006); however, we found that the Gαs-CFP fusion was mostly cytoplasmic, and therefore did not meet our criteria for using it in a FRET biosensor for Gαs activation. We therefore decided to use ^{T}EPAC^{VV}, a unimolecular FRET sensor based on the cAMP-binding domains of the protein Epac1, which can measure Gαs-mediated stimulation in cAMP levels inside cells (Klarenbeek et al., 2011), to measure H_2R activation. The H_3R and H_4R are predominantly linked to the activation of Gαi, which is classically assayed by probing the inhibition of forskolin-stimulated cAMP production in cells (Sensken et al., 2008). To provide a more direct way to measure Gαi, we used a recently developed intermolecular FRET biosensor that directly reports on the activation of Gαi by monitoring the separation of the Gα subunit and the Gγ subunit (van Unen et al., 2016).

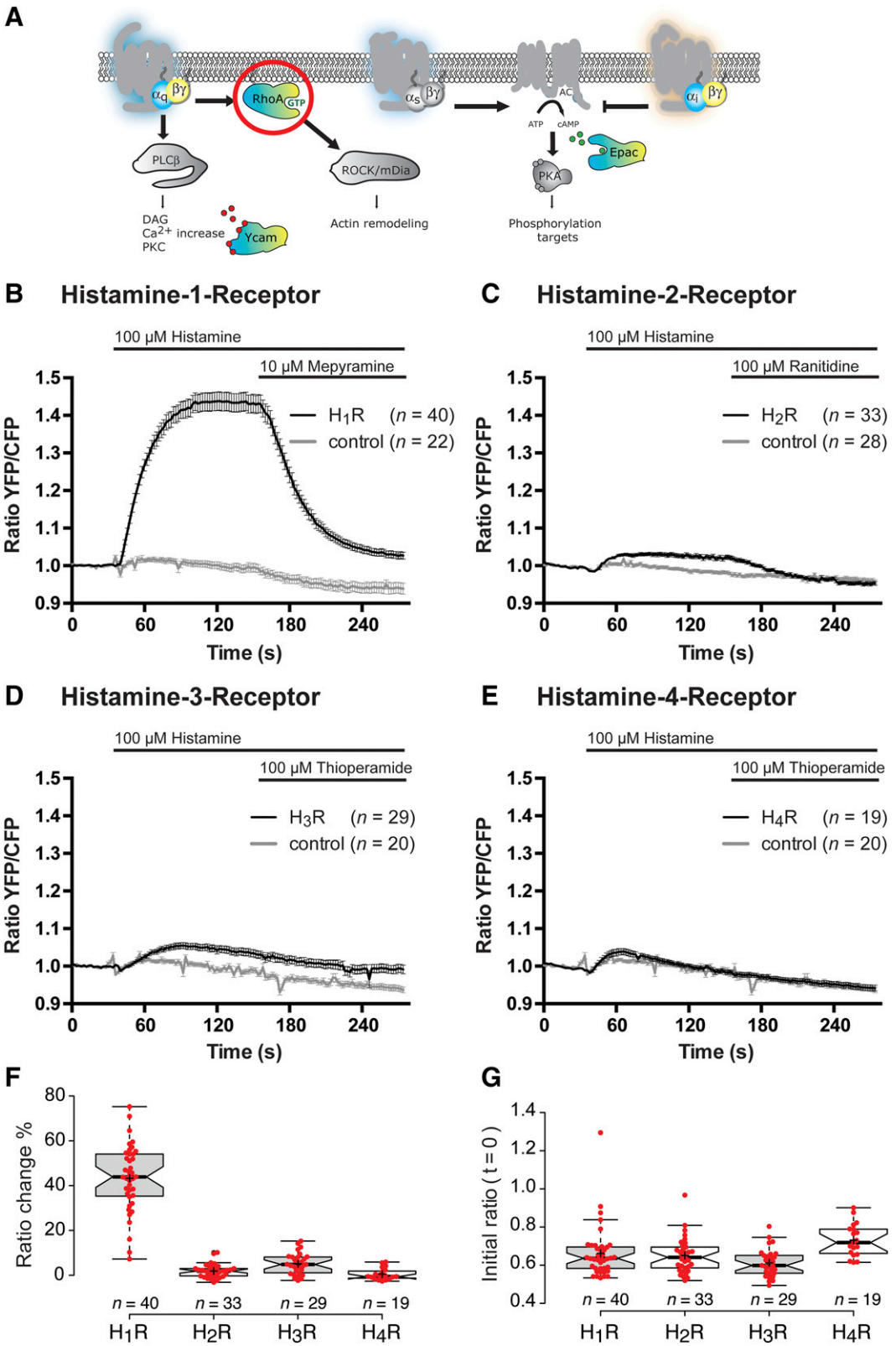

Fig. 4. RhoA signaling by histamine receptors. (A) Activation of the DORA RhoA biosensor by the four histamine receptor subtypes, measured by FRET ratio imaging. (B) Hela cells transfected with H_1R-p2A-RFP and the DORA RhoA biosensor were treated with histamine and mepyramine (black). Control cells were transfected with only the DORA RhoA biosensor (gray). (C) Cells transfected with H_2R-p2A-RFP and the DORA RhoA biosensor were treated with histamine and ranitidine (black). In the control condition, cells were transfected with only the DORA RhoA biosensor (gray). (D) Cells transfected with H_3R-p2A-RFP and the DORA RhoA biosensor were treated with histamine and thioperamide (black). In the control condition, cells were transfected with only the DORA RhoA (gray). (E) Cells transfected with H_4R-p2A-RFP and the DORA RhoA biosensor were treated with histamine and thioperamide (black). In the control condition, cells were transfected with only the DORA RhoA biosensor (gray). The median and average (+) amplitude of the FRET ratio change at t = 100 seconds (F) and the raw YFP/CFP ratio at t = 0 seconds (G) per receptor subtype, quantified from the experiments shown in (B–E). Box limits indicate the

We used these FRET biosensors to measure the signaling responses upon stimulation of the four histamine receptor subtypes to create heterotrimeric G-protein signaling profiles per receptor.

Tagging of Histamine Receptors with a Fluorescent Protein. The four human histamine receptor subtypes were fused to the RFP variant mCherry on their C-terminal end and imaged using confocal microscopy to examine their localization in living cells. The H_1R, H_2R, H_3R, or H_4R was predominantly localized to the plasma membrane (Fig. 2A). Since some of the FRET biosensors used in this study are also localized to the plasma membrane, we anticipated that FRET could occur between fluorescent proteins present in the FRET biosensors and the RFP fused to the C-terminal of the receptor (Fig. 2B, left). To prevent bystander FRET, we used a strategy where the RFP is separated from the receptor protein during translation, and is thus no longer localized to the plasma membrane (Fig. 2B, right). With this strategy, the receptor is essentially untagged, and the RFP can still be used as a reporter for receptor translation. We cloned a previously described p2A sequence (Kim et al., 2011) in between the coding sequences for the receptors and the RFP, resulting in plasmids containing HxR-p2A-RFP (for details, see *Materials and Methods*). As a result, HeLa cells transfected with these constructs showed cytosolic localization of RFP fluorescence, as shown for H_4R-p2A-RFP (Fig. 2C) and the other three histamine receptor subtypes (Supplemental Fig. 1).

Analysis of Gαq Signaling by Four Histamine Receptor Subtypes. To study which of the histamine receptor subtypes is capable of activating the heterotrimeric G-protein Gαq, we performed live cell measurements on HeLa cells transfected with the Gαq biosensor (Fig. 3A) and cotransfected with H_1R-p2A-RFP, H_2R-p2A-RFP, H_3R-p2A-RFP, or H_4R-p2A-RFP. YFP and CFP fluorescence was monitored over time, and cells were stimulated with the indicated amount of agonist and antagonist. Activation of the H_1R was achieved by stimulating the cells at the indicated time points with histamine, and the response was antagonized by the addition of the H_1R-specific antagonist mepyramine (Leurs et al., 1995). A fast drop in YFP/CFP FRET ratio (10–30%) was observed after addition of histamine, indicating a fast activation of the receptor and subsequent separation of Gαq subunit and Gβγ dimer. The signal quickly returned to baseline after addition of mepyramine (Fig. 3B, black trace). No change in YFP/CFP FRET ratio was observed in cells transfected with H_2R, H_3R, or H_4R after stimulation with histamine and subsequent addition of the H_2R-specific antagonist ranitidine (Leurs et al., 1995) or the H_3R/H_4R-specific antagonist thioperamide (Leurs et al., 1995), indicating no activation or deactivation of Gαq by H_2R, H_3R, or H_4R (Fig. 3, C–E, black traces). Cells in control conditions (no GPCR coexpression) were transfected with the Gαq biosensor and did not show any change in FRET ratio upon addition of the relevant agonists and antagonists (Fig. 3, B–E, gray traces). The amplitude of the FRET ratio change at t = 100 seconds, was quantified from single cells per histamine receptor subtype (Fig. 3F). The basal FRET ratio of the biosensors at the start of every experiment (t = 0) was used to evaluate basal activity. We did not observe large differences in FRET ratio between the receptor subtypes at the start of the experiment (Fig. 3G).

From these results, we conclude that only the H_1R effectively couples to the heterotrimeric G-protein Gαq, and this biosensor provides high selectivity and sensitivity to readout H_1R activation.

Analysis of RhoA Signaling by Four Histamine Receptor Subtypes. To study the activation of the small GTPase RhoA, we performed live cell measurements on HeLa cells transfected with the DORA RhoA biosensor (Fig. 4A) and cotransfected with H_1R-p2A-RFP, H_2R-p2A-RFP, H_3R-p2A-RFP, or H_4R-p2A-RFP. Activation of the H_1R resulted in a fast increase in YFP/CFP FRET ratio (30–60%), indicating a fast activation of the receptor and subsequent exchange of GTP for GDP on the RhoA biosensor. The signal rapidly returned to baseline after addition of mepyramine (Fig. 4B, black trace). Activation of the H_2R resulted in a small reversible change in YFP/CFP FRET ratio (5%) (Fig. 4C, black trace). Activation of the H_3R resulted in a slow, small transient change in YFP/CFP FRET ratio, whereas no change in YFP/CFP FRET ratio was observed after activation of the H_4R (Fig. 3, D and E, black traces). Cells in the control condition that were transfected with the DORA RhoA biosensor showed a minor reversible change in FRET ratio (<5%) upon addition of histamine (Fig. 4, B–E, gray traces). We observed this small response previously (van Unen et al., 2015a), and it can most likely be attributed to the activation of the endogenous guanine exchange factor trio (van Rijssel and van Buul, 2012) by endogenous H_1R receptors. We repeated this experiment in human embryonic kidney 293 (HEK293) cells, which do not contain endogenous H_1R receptors, and found similar results for the activation of RhoA by ectopically expressed H_1R, but no change in YFP/CFP FRET ratio for the control condition (Supplemental Fig. 2).

The amplitude of the FRET ratio change at t = 100 seconds (Fig. 4F) and the start ratio (Fig. 4G) were quantified from single cells per histamine receptor to allow comparison between the receptor subtypes.

From these results, we conclude that the H_1R effectively signals to the small GTPase RhoA. The small effects of the H_2R and H_3R on the DORA RhoA biosensor that were observed are possibly mediated by a minor activation of endogenous Gαq or Gα12/Gα13 by these receptors.

Analysis of Calcium Signaling by Four Histamine Receptor Subtypes. To investigate changes in intracellular Ca^{2+} concentration upon stimulation of the four histamine receptor subtypes, we performed live cell measurements on HEK293 cells transfected with the Ycam biosensor (Fig. 5A) and cotransfected with H_1R-p2A-RFP, H_2R-p2A-RFP, H_3R-p2A-RFP, or H_4R-p2A-RFP. HEK293 cells were used in this experiment because endogenous H_1 receptors in HeLa cells interfere with the measurements of intracellular Ca^{2+}. Carbachol was added at the indicated time points to stimulate

25th and 75th percentiles as determined by R software; whiskers extend 1.5 times the interquartile range from the 25th and 75th percentiles. HeLa cells were stimulated with histamine at *t* = 32 seconds, and the response was antagonized by the addition of the appropriate antagonist at *t* = 152 seconds. Time traces show the average ratio change of YFP/CFP fluorescence (± S.E.M.). AC, adenylyl cyclase; DAG, diacylglycerol; mDia, mammalian diaphanous-related formin 1; PKA, protein kinase A; PKC, protein kinase C; ROCK, Rho-associated coiled-coil-containing protein kinase.

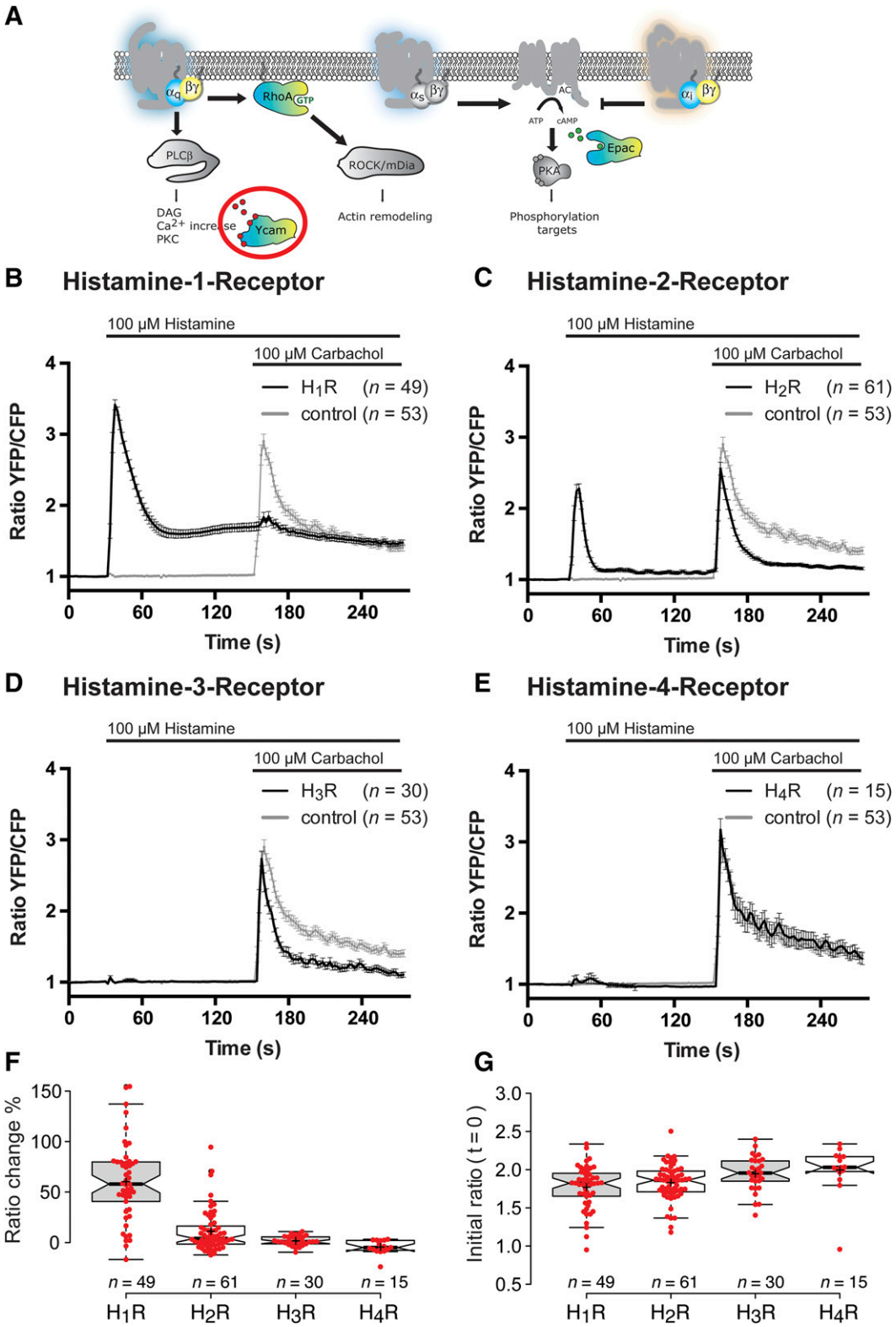

Fig. 5. Calcium signaling by histamine receptors. (A) Activation of the Ycam calcium biosensor by the four histamine receptor subtypes, measured by FRET ratio. (B) HEK293 cells transfected with H_1R-p2A-RFP and the Ycam biosensor were treated with histamine and carbachol (black). Control cells transfected with only the Ycam biosensor were treated with histamine and carbachol (gray). This control condition is the same for all receptor subtypes in this experiment. (C) Cells transfected with H_2R-p2A-RFP and the Ycam biosensor were treated with histamine and carbachol (black). (D) Cells transfected with H_3R-p2A-RFP and the Ycam biosensor were treated with histamine and carbachol (black). (E) Cells transfected with H_4R-p2A-RFP and the Ycam were treated with histamine and carbachol (black). The median and average (+) amplitude of the FRET ratio change at t = 100 seconds (F) and the raw YFP/CFP ratio at t = 0 seconds (G) per receptor subtype, quantified from the experiments shown in (B–E). Box limits indicate the 25th and 75th percentiles as determined by R software; whiskers extend 1.5 times the interquartile range from the 25th and 75th percentiles. HEK293 cells were stimulated with histamine at t = 32 seconds and stimulated with carbachol at t = 152 seconds. Time traces show the average ratio change of YFP/CFP fluorescence (± S.E.M.). AC, adenylyl cyclase; DAG, diacylglycerol; mDia, mammalian diaphanous-related formin 1; PKA, protein kinase A; PKC, protein kinase C; ROCK, Rho-associated coiled-coil-containing protein kinase.

endogenous M_1/M_3 receptors as a positive endpoint control for intracellular Ca^{2+} release (Zhu et al., 1998). Stimulation of the H_1R resulted in a fast transient increase in YFP/CFP FRET ratio (300–400%), which is indicative of a rise in intracellular calcium. The signal decreased and stabilized again at an elevated ratio compared with baseline (Fig. 5B, black trace). Stimulation with carbachol did not further change the YFP/CFP ratio, suggesting depletion of intracellular Ca^{2+} stores upon histamine stimulation or desensitization of Gαq signaling. Interestingly, we observed a fast transient increase in YFP/CFP FRET ratio (200–300%) upon stimulation of the H_2R (Fig. 5C, black trace). Subsequent stimulation with carbachol resulted in a similar fast transient increase in YFP/CFP FRET ratio (200–300%). This indicates that activation of the H_2R causes release of intracellular Ca^{2+}. Preincubation with the specific Gαq inhibitor FR900359 (Schrage et al., 2015) resulted in a complete abrogation of intracellular Ca^{2+} release in response to either H_2R activation or carbachol stimulation (Supplemental Fig. 3). These results show that Gαq mediates intracellular Ca^{2+} release downstream of H_2R, either directly or indirectly. Gαq-mediated Ca^{2+} release is a process that involves multiple steps that amplify the response (Berridge et al., 2000). This may explain why, after H_2R activation, the response of the Gαq biosensor remains under the threshold of detection, but still leads to robust calcium release.

Activation of the H_3R or H_4R did not result in a change of YFP/CFP FRET ratio (Fig. 5, D and E, black traces). In control cells transfected with Ycam, we did not observe a change in YFP/CFP FRET ratio upon stimulation with histamine, but stimulation with carbachol resulted in a transient increase in YFP/CFP FRET ratio (250–350%) (Fig. 5, B–E, gray traces).

The amplitude of the FRET ratio change at t = 100 seconds was quantified from single cells per histamine receptor subtype (Fig. 5F). We did not observe large differences in basal FRET ratio between the receptor subtypes (Fig. 5G).

From this, we conclude that activation of the H_1R and, surprisingly, the H_2R leads to release of intracellular Ca^{2+}, providing evidence for Gαq coupling at both of these receptors.

Analysis of cAMP Signaling by Four Histamine Receptor Subtypes. To assess the production of cAMP upon stimulation of the four histamine receptor subtypes, we performed live cell measurements on HeLa cells transfected with the $^{T}EPAC^{VV}$ biosensor (Fig. 6A) and cotransfected with H_1R-p2A-RFP, H_2R-p2A-RFP, H_3R-p2A-RFP, or H_4R-p2A-RFP. The $^{T}EPAC^{VV}$ biosensor is a loss-of-FRET sensor displaying a decrease in YFP/CFP ratio when cAMP levels are increased (Klarenbeek et al., 2011). Stimulation of the H_1R resulted in a small reversible change in the YFP/CFP FRET ratio (5–15%), indicating a small transient increase in cAMP levels (Fig. 6B, black trace). Stimulation of cells expressing the H_1R, preincubated with either the inhibitor for Gαq (FR900359) (Schrage et al., 2015) or the specific inhibitor for Gαi family proteins (PTX) (Burns, 1988), evoked a similar response on cAMP production, excluding Gαq- or Gαi-mediated effects (Supplemental Fig. 4B). Stimulation of the H_2R resulted in a substantial and reversible change in YFP/CFP FRET ratio (40–60%) (Fig. 6C, black trace). Stimulation of HEK293 cells transfected with the H_2R resulted in a similar change in YFP/CFP FRET ratio (40–70%), which was not visibly reversible by ranitidine, possibly due to an oversaturation effect of the biosensor (Supplemental Fig. 4A, black trace). Interestingly, stimulation of HEK293 cells with only $^{T}EPAC^{VV}$ transfection resulted in a transient change of YFP/CFP FRET ratio (10–30%), which was sensitive to ranitidine addition, a strong indication for the endogenous presence of H_2R receptors in HEK293 cells (Supplemental Fig. 4A, gray trace). Stimulation of the H_3R or H_4R did not result in any change in YFP/CFP FRET ratio, indicating no changes in basal cAMP levels (Fig. 6, D and E, black traces). In control cells transfected with $^{T}EPAC^{VV}$, we did not observe a change in YFP/CFP FRET ratio upon stimulation with histamine or any of the antagonists (Fig. 6, B–E, gray traces). The amplitude of the FRET ratio change at t = 100 seconds was quantified from single cells per histamine receptor subtype (Fig. 6F) as well as the FRET ratio at the start of the experiment (Fig. 6G).

From these results, we conclude that the H_2R strongly induces cAMP production, whereas the experiments with H_1R suggest a minor effect on cAMP production, presumably via coupling to Gαs.

Analysis of Gαi Signaling by Four Histamine Receptor Subtypes. To study the activation of the heterotrimeric G-protein Gαi_1, we performed live cell measurements on HeLa cells transfected with a previously published Gαi_1 biosensor (van Unen et al., 2016) (Fig. 7A) and cotransfected with H_1R-p2A-RFP, H_2R-p2A-RFP, H_3R-p2A-RFP, or H_4R-p2A-RFP. Stimulation of the H_1R resulted in fast reversible change in YFP/CFP FRET ratio (10–20%). Overnight preincubation of cells with PTX completely abrogated this response, further strengthening the evidence for activation of Gαi_1 by H_1R (Supplemental Fig. 5). Stimulation of the H_2R did not result in a change in YFP/CFP FRET ratio. Stimulation of the H_3R and H_4R resulted in a fast, partly reversible change in YFP/CFP FRET ratio (10–20%). Stimulation of control cells transfected with only the Gαi_1 biosensor did not result in a change in YFP/CFP FRET ratio (Fig. 7, B–E, gray traces). The amplitude of the FRET ratio change at t = 100 seconds was quantified from single cells per histamine receptor subtype, showing clear activation of the Gαi_1 biosensor by subtypes H_1R, H_3R, and H_4R (Fig. 7F). We did not observe large differences in basal FRET ratio between the receptor subtypes (Fig. 7G).

These results led us to conclude that the H_1R, H_3R, and H_4R can robustly couple to and activate the heterotrimeric G-protein Gαi_1.

Single-Cell Analysis of Pharmacological Parameters with FRET-Based Biosensors

Based on the systematic interrogation with FRET biosensors that measure the activation of different G-protein families in this study, we propose a revision of G-protein selectivity at the four histamine receptor subtypes (summarized in Fig. 8A).

Finally, we tested whether FRET-based biosensors can be used to determine important pharmacological parameters, including antagonist specificity and concentration-response curves. To demonstrate the application of a FRET sensor for the rapid testing of multiple antagonists, we transfected HeLa cells with the $^{T}EPAC^{VV}$ biosensor and cotransfected with H_2R-p2A-RFP. Cells were sequentially stimulated with histamine, mepyramine, thioperamide, and ranitidine at the indicated time points (Fig. 8B). Histamine addition resulted in an expected

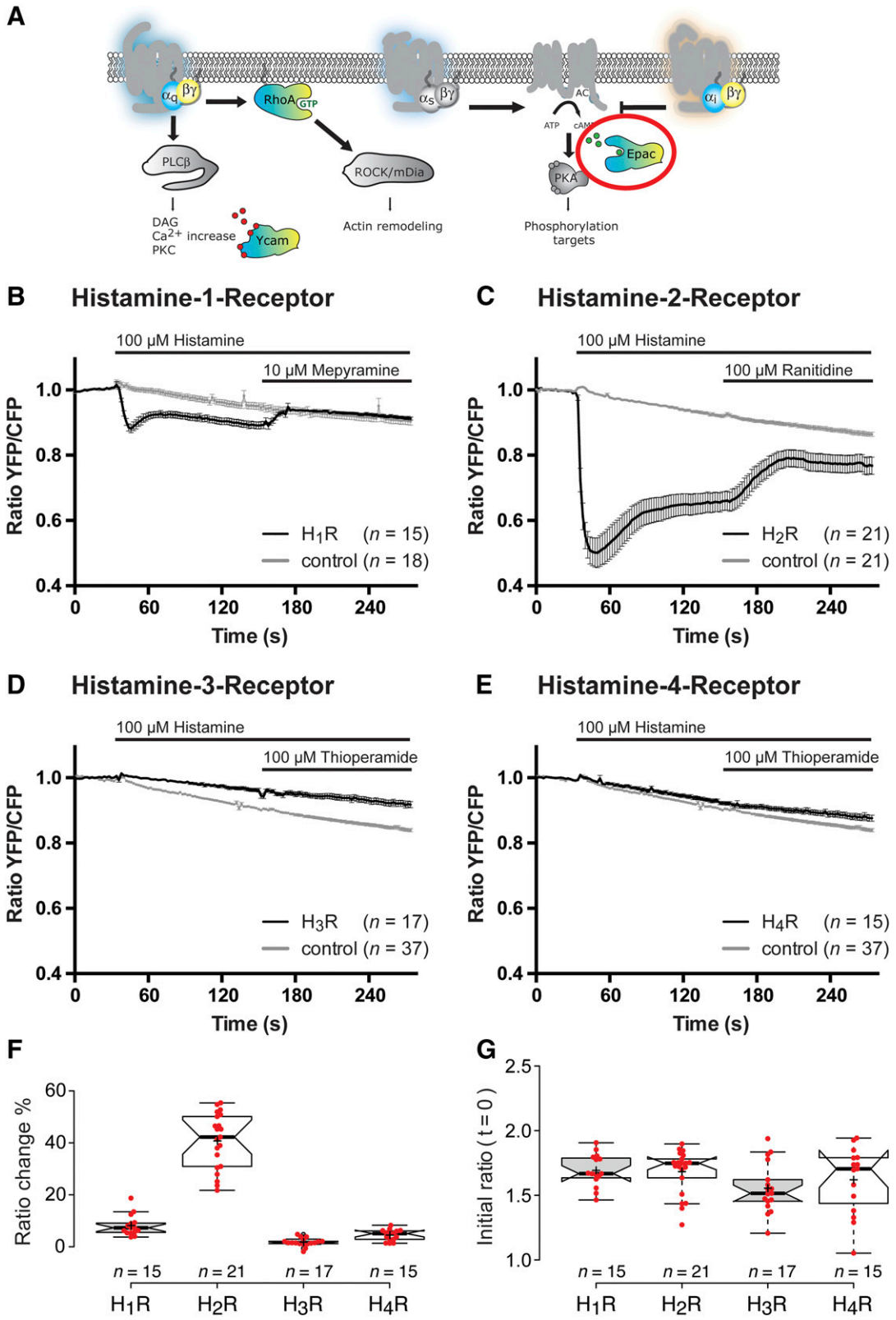

Fig. 6. cAMP signaling by histamine receptors. (A) Production of cAMP by the four histamine receptor subtypes visualized by the ^{T}EPAC^{VV} biosensor and measured by FRET ratio. (B) Hela cells transfected with H_1R-p2A-RFP and the ^{T}EPAC^{VV} biosensor were treated with histamine and mepyramine (black). Control cells were transfected with only the ^{T}EPAC^{VV} biosensor (gray). (C) Cells transfected with H_2R-p2A-RFP and the ^{T}EPAC^{VV} biosensor were treated with histamine and ranitidine (black). Control cells were transfected with only the ^{T}EPAC^{VV} biosensor (gray). (D) Cells transfected with H_3R-p2A-RFP and the ^{T}EPAC^{VV} biosensor were treated with histamine and thioperamide (black). In the control condition, cells were transfected with only the ^{T}EPAC^{VV} biosensor (gray). (E) Cells transfected with H_4R-p2A-RFP and the ^{T}EPAC^{VV} biosensor were treated with histamine and thioperamide (black). In the control condition, cells were transfected with only the ^{T}EPAC^{VV} biosensor (gray). The median and average (+) amplitude of the FRET ratio change at t = 100 seconds (F) and the raw YFP/CFP ratio at t = 0 seconds (G) per receptor subtype, quantified from the experiments shown in (B–E). Box limits

fast drop in YFP/CFP ratio (40–60%), and only upon addition of ranitidine did the ratio partly return to baseline levels, showing the specific inhibition of the H_2R by ranitidine. To explore the possibility of using FRET sensors for single-cell concentration-response curves, we transfected HeLa cells with H_1R-p2A-RFP and the Gαq biosensor, the Gαi_1 biosensor, or the DORA RhoA biosensor. Titration of increasing amounts of histamine resulted in concentration-response curves with pEC_{50} values of 6.05 [95% confidence interval (CI), 6.21–5.88] for Gαq activation (Fig. 8C), 5.07 (95% CI, 5.63–4.50) for RhoA activation (Fig. 8D), and 5.05 (95% CI, 5.78–4.33) for Gαi_1 activation (Fig. 8E).

Next, we evaluated the effect of a potent synthetic H_1R ligand, methylhistaprodifen (Elz et al., 2000), on Gαq versus Gαi_1 activation. The concentration-response curves yielded pEC_{50} values of 6.50 (95% CI, 6.71–6.27) for Gαq activation (Fig. 8C) and 5.30 (95% CI, 6.53–4.07) for Gαi_1 activation (Fig. 8E). The extent of Gαi_1 activation by methylhistaprodifen was attenuated relative to histamine.

To assess the potency of the H_3R and H_4R for the activation of Gαi_1, we transfected HeLa cells with the Gαi_1 biosensor and the H_3R-p2A-RFP or H_4R-p2A-RFP. We found pEC_{50} values of 7.71 (95% CI, 7.94–7.48) and 8.09 (95% CI, 8.28–7.91) for the H_3R and H_4R, respectively (Fig. 8F). When we titrated increasing histamine concentrations in cells transfected with H_2R-p2A-RFP and the $^{T}EPAC^{VV}$ biosensor, we observed a transient full response on $^{T}EPAC^{VV}$ even at the lowest concentrations used, which rendered the data unsuitable for concentration-response curve analysis (for raw YFP/CFP ratio traces, see Supplemental Fig. 6). From these data, we conclude that FRET biosensors can be used to assess antagonist specificity at receptors, and that they can be used to obtain single-cell concentration-response curves.

Discussion

Using several biosensors based on FRET, we have characterized the canonical G-protein–coupled signaling profiles of the four histamine receptors. Our results provide evidence that, besides the well known activation of Gαq, the H_1R can also couple efficiently to Gαi_1 proteins, in agreement with previously published results (Murayama et al., 1990; Seifert et al., 1994). We also found a small increase in cAMP production following H_1R activation, which provides evidence toward Gαs coupling via H_1R. Activation of the H_2R greatly increased the production of cAMP, which was described previously, but surprisingly we also found a Gαq-mediated increase in Ca^{2+} upon stimulation of this receptor. The H_3R and H_4R seem to couple exclusively to Gαi_1 proteins, which is in good agreement with the literature. The absence of Ca^{2+} release by H_3R and H_4R indicates that G$\beta\gamma$-mediated activation of PLC, which is strongly cell-type dependent, is not effective under our conditions (Khan et al., 2013). Moreover, the experiments presented in this paper show that FRET biosensors can be used to examine antagonist specificity and potency of GPCR ligands. It must be noted that we did not assess the specific activation of Gα12/Gα13 proteins by histamine receptors, as robust and specific FRET sensors for this G-protein family do not exist yet. Still, we expect that Gα12/Gα13 activity can be picked up by the DORA RhoA sensor, and it can be separated from a Gαq response by using the specific Gαq inhibitor FR900359. The H_1R-mediated activation of RhoA has been described in detail before and is specifically induced by Gαq (van Unen et al., 2015a), but we cannot exclude the possibility that the small responses on the DORA RhoA biosensor after H_2R and H_3R activation are partly mediated by Gα12/Gα13 activation.

Previously, we determined that, under similar experimental conditions, HeLa cells have 710 fmol/mg binding sites for H_1R (Adjobo-Hermans et al., 2011), which corresponds roughly to 680,000 receptors per cell at a 25% transfection efficiency (assuming a cell volume of 2 pl and a protein concentration of 0.2 mg/ml). We did not notice differences in fluorescence levels between the four different isoforms in this study, either when directly tagged or in the case of a cotranslated mCherry. We note that the fluorescence intensity of the cotranslated mCherry can be used as a measure for receptor level since the 2A peptide produces two proteins in a 1:1 stoichiometry.

Although not explored in this work, FRET biosensors are also very well suited to report spatial signaling information, which can be used to distinguish signaling at the plasma membrane (G-protein activation) from signaling in the cytosol (cAMP production/Ca^{2+} release) or other subcellular locations (Piljić and Schultz, 2008). Given the recent reports on intracellular GPCR signaling (Vilardaga et al., 2014; Tsvetanova et al., 2015), this would be an interesting avenue to explore for, e.g., the H_2R with FRET biosensors in future studies.

There are multiple benefits of using FRET sensors over conventional biochemical assays to measure G-protein signaling. Ligand binding and unbinding kinetics can be determined with high temporal resolution (Lohse et al., 2012; van Unen et al., 2016), and concentration-response curve measurements can be obtained from single cells in real time, revealing cell-to-cell heterogeneity (e.g., Figs. 3–7, F and G). Specifically, the Gαi FRET biosensors measure Gαi activation in a more relevant cellular state than the classic biochemical assays that require forskolin-induced cAMP production. On the other hand, population-based methods allow for a higher throughput.

Furthermore, FRET biosensors can be multiplexed, meaning that multiple signaling readouts can be measured at the same time in the same single cell (Piljić and Schultz, 2008). A related approach is to combine information on the FRET biosensor readouts with spatial and temporal information on cell shape or cell behavior (van Unen et al., 2015a). The combination of FRET biosensors and microfluidics approaches (Martins et al., 2012; Sackmann et al., 2014) can be used to solve more detailed questions around GPCRs by delivering more precisely defined stimulations to cells (for example, repeated stimuli or gradients).

indicate the 25th and 75th percentiles as determined by R software; whiskers extend 1.5 times the interquartile range from the 25th and 75th percentiles. HeLa cells were stimulated with histamine at t = 32 seconds, and the response was antagonized by the addition of the appropriate antagonist at t = 152 seconds. Time traces show the average ratio change of YFP/CFP fluorescence (± S.E.M.). AC, adenylyl cyclase; DAG, diacylglycerol; mDia, mammalian diaphanous-related formin 1; PKA, protein kinase A; PKC, protein kinase C; ROCK, Rho-associated coiled-coil-containing protein kinase.

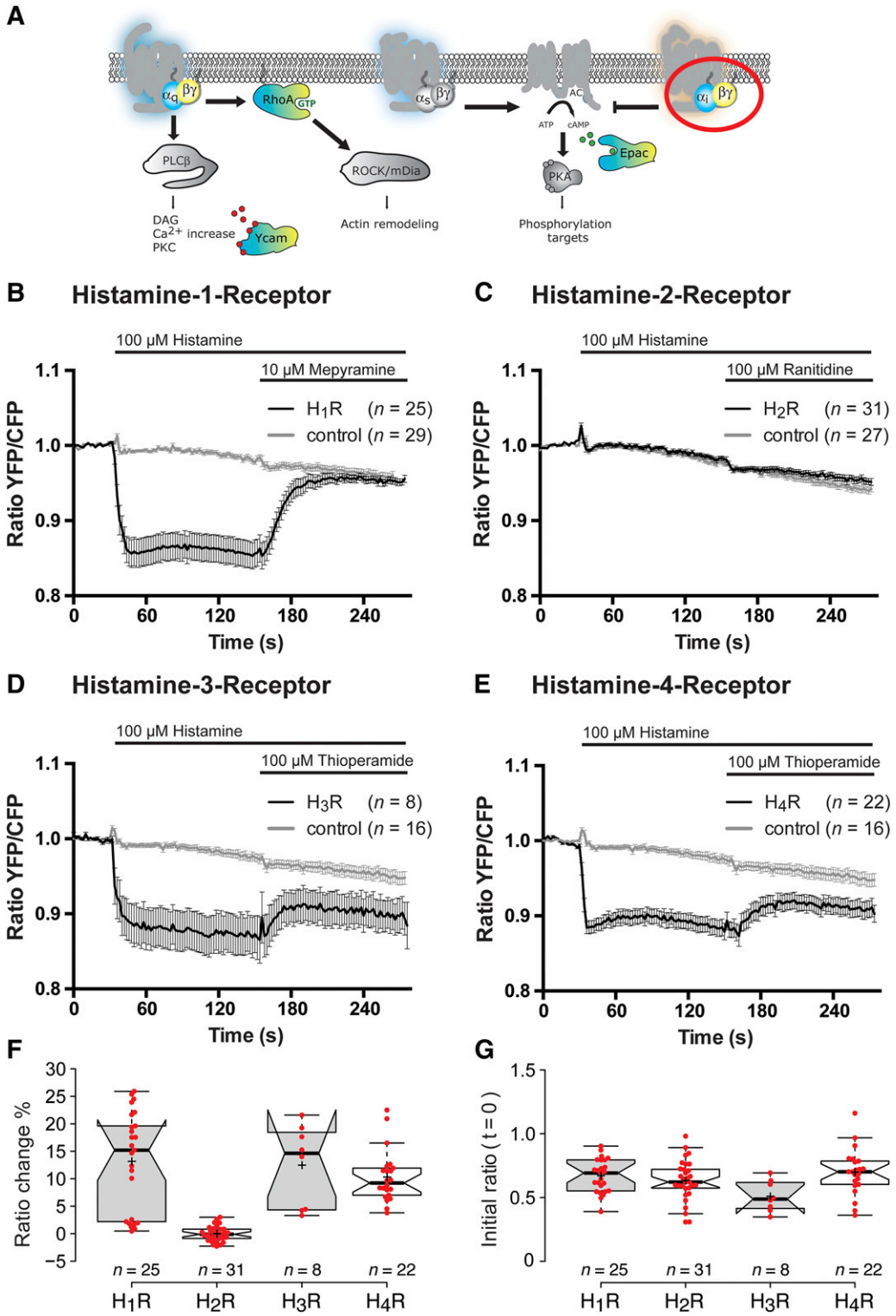

Fig. 7. Gαi signaling by histamine receptors. (A) Activation of the heterotrimeric G-protein Gαi by the four histamine receptor subtypes, as measured by FRET ratio. (B) Hela cells transfected with H_1R-p2A-RFP and the Gαi biosensor were treated with histamine and mepyramine (black). Control cells were transfected with only the Gαi biosensor (gray). (C) Cells transfected with H_2R-p2A-RFP and the Gαi biosensor were treated with histamine and ranitidine (black). In the control condition, cells were transfected with only the Gαi biosensor (gray). (D) Cells transfected with H_3R-p2A-RFP and the Gαi biosensor were treated with histamine and thioperamide (black). In the control condition, cells were transfected with only the Gαi biosensor (gray). (E) Cells transfected with H_4R-p2A-RFP and the Gαi biosensor were treated with histamine and thioperamide (black). In the control condition, cells were transfected with only the Gαi biosensor (gray). The median and average (+) amplitude of the FRET ratio change at t = 100 seconds (F) and the raw YFP/CFP ratio at t = 0 seconds (G) per receptor subtype, quantified from the experiments shown in (B–E). Box limits indicate the 25th and 75th percentiles as determined by R software; whiskers extend 1.5 times the interquartile range from the 25th and 75th percentiles. HeLa cells were stimulated with histamine at t = 32 seconds, and the response was antagonized by the addition of the appropriate antagonist at t = 152 seconds. Time traces show the average ratio change of YFP/CFP fluorescence (± S.E.M.). AC, adenylyl cyclase; DAG, diacylglycerol; mDia, mammalian diaphanous-related formin 1; PKA, protein kinase A; PKC, protein kinase C; ROCK, Rho-associated coiled-coil-containing protein kinase.

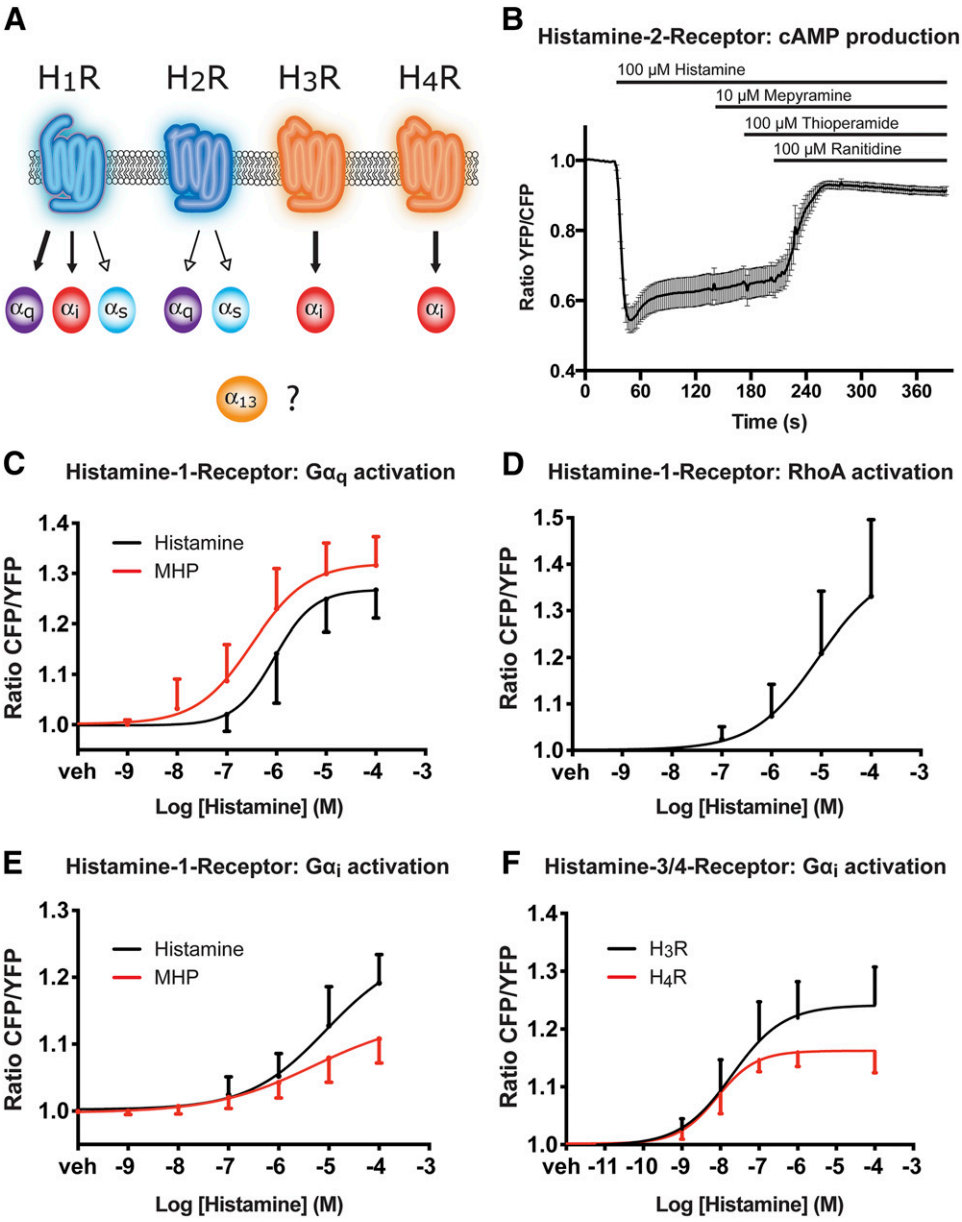

Fig. 8. Single-cell pharmacology using FRET biosensors. (A) Schematic overview of proposed G-protein selectivity at the four histamine receptor subtypes, based on the findings in this study. Open arrowheads indicate either direct or indirect activation. (B) HeLa cells transfected with H_2R-p2A-RFP and the $^{T}EPAC^{VV}$ biosensor were stimulated with histamine (t = 32) and subsequently stimulated with mepyramine (t = 132), thioperamide (t = 172), and ranitidine (t = 212) (n = 21). Time traces show the average ratio change of YFP/CFP fluorescence (± S.E.M.). (C) Concentration-response curve showing the change in CFP/YFP ratio in HeLa cells transfected with the H_1R-p2A-RFP and the Gαq biosensor upon titration of increasing amounts of histamine (black line, n = 26) or methylhistaprodifen (MHP) (red line, n = 17). (D) Concentration-response curve showing the change in YFP/CFP ratio upon titration of increasing amounts of histamine in HeLa cells transfected with the H_1R-p2A-RFP and the DORA RhoA biosensor (n = 33). (E) Concentration-response curve showing the change in CFP/YFP ratio in HeLa cells transfected with the H_1R-p2A-RFP and the Gαi biosensor upon titration of increasing amounts of histamine (black line, n = 17) or methylhistaprodifen (red line, n = 10). (F) Concentration-response curve showing the change in CFP/YFP ratio upon titration of increasing amounts of histamine in HeLa cells transfected with either the H_3R-p2A-RFP (n = 29) or H_4R-p2A-RFP (n = 16) and the Gαi biosensor. HeLa cells in (C–E) were sequentially stimulated with cumulative concentrations of 100 nM, 1 μM, 10 μM and 100 μM histamine or 1 nM, 10 nM, 100 nM, 1 μM, 10 μM and 100 μM methylhistaprofiden. HeLa cells in (F) were sequentially stimulated with cumulative concentrations of 1 nM, 10 nM, 100 nM, 1 μM, and 100 μM histamine. Error bars in (C–F) depict S.D.

We demonstrate that the contrast of several existing FRET biosensors is sufficient to use them for real-time single-cell analysis. Whether these FRET-based sensors provide sufficient sensitivity for high-throughput cell-based screening remains to be investigated.

A general limitation of (FRET-based) biosensors is the buffering or amplification of signals by the overexpressed biosensors. This is especially relevant at longer timescales when the signals are part of feedback or feedforward loops. This can be prevented by limiting the expression levels and measuring for short time periods.

A specific limitation of the Gαq and Gαi FRET biosensors is that they depend on overexpression of the heterotrimer, which possibly affects the natural coupling preference of the GPCR for certain classes of G-proteins. Future studies using gene-editing techniques such as CRISPR-Cas9 (Lackner et al., 2015) can overcome this limitation by tagging the endogenous subunits with fluorescent proteins instead.

A small percentage of the HEK293 control cells (5%) in the calcium release experiment show a response on the Ycam biosensor after the first stimulation with histamine. This possibly represents a Gαq-mediated response in cells that have a high expression of endogenous H_2R. There is conflicting evidence about endogenously expressed histamine receptors in HEK293 cells (Iwata et al., 2005; Atwood et al., 2011). A possible explanation could be that this Gαq-mediated response is due to the recently found heterodimerization or cross-talk of possible endogenous H_1R and the ectopically expressed H_2R (Alonso et al., 2013), which could also provide an alternative explanation for the results of the $^{T}EPAC^{VV}$ biosensor presented in Supplemental Fig. 4A.

The different additions of the concentration-response curves in our experiments are cumulatively added to cells. Because of the repeated stimulation regimen, desensitization effects or receptor internalization events could take place during our experiments. However, our obtained pEC_{50} values for histamine

at the H_1R (6.05), H_3R (7.71), and H_4R (8.09) compare well to previously published pEC_{50} values obtained in GTPase assays in Sf9 insect cells (Seifert et al., 2013).

The concentration-response curves obtained with methylhistaprodifen show a preference of Gαq over Gαi when compared with the natural ligand histamine, suggesting ligand-biased signaling. Whether such a preference is conveyed to downstream signaling and a different physiologic outcome will be an interesting future direction.

Internal calcium release, as measured by the Ycam FRET biosensor, leads to a fast transient calcium spike in receptor overexpression conditions when stimulated with saturating agonist concentration. The measured responses after endogenous receptor stimulation (carbachol in our experiments) can differ vastly from oscillatory behavior in various frequencies to a single or multiple sparsely distributed spikes. Because of the extreme heterogeneity in responses, the all-or-nothing response pattern for overexpressed receptors, and the many factors that can contribute to the calcium signal (Berridge et al., 2000), we deemed these measurements not suitable for the generation of concentration-response curves. Similarly, we observed a transient response for the cAMP biosensor, hindering the determination of the potency of the H_2R. In general, a requirement for obtaining concentration-response curves from single-cell data is that the response of the biosensor reaches a plateau on a timescale of seconds. This seems to be a general feature of the heterotrimeric G-protein biosensors, highlighting the need for this kind of FRET sensor for Gαs and Gα12/Gα13.

In conclusion, we characterized the canonical G-protein signaling profiles of the four histamine receptor subtypes using FRET biosensors. Moreover, we show that it is feasible to produce concentration-response curves from single-cell measurements, and that FRET biosensors can be used to screen for antagonist specificity. We expect that FRET-based biosensor measurements provide a valuable addition to the existing palette of quantitative cell-based methods for measuring GPCR activation.

Acknowledgments

The authors thank H. Vischer (VU University) for providing cDNA encoding H_4R, and A. Pietraszewska (University of Amsterdam) for the cloning of N1-H_4R-mCherry and N1-H_4R-p2A-mCherry. We are grateful to Y. Wu (UConn Health, Farmington, CT) for sharing the DORA RhoA sensor, and to Andrea Strasser and Sigurd Elz (Universität Regensburg, Germany) for providing methylhistaprodifen. The authors thank Carsten Hoffmann (University of Würzburg, Würzburg, Germany) for critically reading the manuscript.

Authorship Contributions

Participated in research design: van Unen, Postma, Gadella, Goedhart.

Conducted experiments: van Unen, Rashidfarrokhi.

Performed data analysis: van Unen, Hoogendoorn, Postma, Goedhart.

Wrote or contributed to the writing of the manuscript: van Unen, Rashidfarrokhi, Hoogendoorn, Postma, Gadella, Goedhart.

References

Adjobo-Hermans MJW, Goedhart J, van Weeren L, Nijmeijer S, Manders EMM, Offermanns S, and Gadella TWJ, Jr (2011) Real-time visualization of heterotrimeric G protein Gq activation in living cells. *BMC Biol* **9**:32.

Alonso N, Fernandez N, Notcovich C, Monczor F, Simaan M, Baldi A, Gutkind JS, Davio C, and Shayo C (2013) Cross-desensitization and cointernalization of H1 and H2 histamine receptors reveal new insights into histamine signal integration. *Mol Pharmacol* **83**:1087–1098.

Atwood BK, Lopez J, Wager-Miller J, Mackie K, and Straiker A (2011) Expression of G protein-coupled receptors and related proteins in HEK293, AtT20, BV2, and N18 cell lines as revealed by microarray analysis. *BMC Genomics* **12**:14.

Berridge MJ, Lipp P, and Bootman MD (2000) The versatility and universality of calcium signalling. *Nat Rev Mol Cell Biol* **1**:11–21.

Bongers G, de Esch I, and Leurs R (2010) Molecular pharmacology of the four histamine receptors. *Adv Exp Med Biol* **709**:11–19.

Burns DL (1988) Subunit structure and enzymic activity of pertussis toxin. *Microbiol Sci* **5**:285–287.

Clister T, Mehta S, and Zhang J (2015) Single-cell analysis of G-protein signal transduction. *J Biol Chem* **290**:6681–6688.

Elz S, Kramer K, Pertz HH, Detert H, ter Laak AM, Kühne R, and Schunack W (2000) Histaprodifens: synthesis, pharmacological in vitro evaluation, and molecular modeling of a new class of highly active and selective histamine H(1)-receptor agonists. *J Med Chem* **43**:1071–1084.

Goedhart J and Gadella TWJ, Jr (2005) Analysis of oligonucleotide annealing by electrophoresis in agarose gels using sodium borate conductive medium. *Anal Biochem* **343**:186–187.

Gulyás G, Tóth JT, Tóth DJ, Kurucz I, Hunyady L, Balla T, and Várnai P (2015) Measurement of inositol 1,4,5-trisphosphate in living cells using an improved set of resonance energy transfer-based biosensors. *PLoS One* **10**:e0125601.

Hein P, Frank M, Hoffmann C, Lohse MJ, and Bünemann M (2005) Dynamics of receptor/G protein coupling in living cells. *EMBO J* **24**:4106–4114.

Hein P, Rochais F, Hoffmann C, Dorsch S, Nikolaev VO, Engelhardt S, Berlot CH, Lohse MJ, and Bünemann M (2006) Gs activation is time-limiting in initiating receptor-mediated signaling. *J Biol Chem* **281**:33345–33351.

Inoue A, Ishiguro J, Kitamura H, Arima N, Okutani M, Shuto A, Higashiyama S, Ohwada T, Arai H, and Makide K et al. (2012) TGFα shedding assay: an accurate and versatile method for detecting GPCR activation. *Nat Methods* **9**: 1021–1029.

Iwata K, Luo J, Penn RB, and Benovic JL (2005) Bimodal regulation of the human H1 histamine receptor by G protein-coupled receptor kinase 2. *J Biol Chem* **280**: 2197–2204.

Jablonowski JA, Carruthers NI, and Thurmond RL (2004) The histamine H4 receptor and potential therapeutic uses for H4 ligands. *Mini Rev Med Chem* **4**: 993–1000.

Janetopoulos C, Jin T, and Devreotes P (2001) Receptor-mediated activation of heterotrimeric G-proteins in living cells. *Science* **291**:2408–2411.

Khan SM, Sleno R, Gora S, Zylbergold P, Laverdure J-P, Labbé J-C, Miller GJ, and Hébert TE (2013) The expanding roles of Gβγ subunits in G protein-coupled receptor signaling and drug action. *Pharmacol Rev* **65**:545–577.

Kim JH, Lee S-R, Li L-H, Park H-J, Park J-H, Lee KY, Kim M-K, Shin BA, and Choi S-Y (2011) High cleavage efficiency of a 2A peptide derived from porcine teschovirus-1 in human cell lines, zebrafish and mice. *PLoS One* **6**:e18556.

Klarenbeek J, Goedhart J, van Batenburg A, Groenewald D, and Jalink K (2015) Fourth-generation epac-based FRET sensors for cAMP feature exceptional brightness, photostability and dynamic range: characterization of dedicated sensors for FLIM, for ratiometry and with high affinity. *PLoS One* **10**:e0122513.

Klarenbeek JB, Goedhart J, Hink MA, Gadella TWJ, and Jalink K (2011) A mTurquoise-based cAMP sensor for both FLIM and ratiometric read-out has improved dynamic range. *PLoS One* **6**:e19170.

Kroeze WK, Sassano MF, Huang X-P, Lansu K, McCorvy JD, Giguère PM, Sciaky N, and Roth BL (2015) PRESTO-Tango as an open-source resource for interrogation of the druggable human GPCRome. *Nat Struct Mol Biol* **22**:362–369.

Lackner DH, Carré A, Guzzardo PM, Banning C, Mangena R, Henley T, Oberndorfer S, Gapp BV, Nijman SMB, and Brummelkamp TR et al. (2015) A generic strategy for CRISPR-Cas9-mediated gene tagging. *Nat Commun* **6**:10237.

Leurs R, Smit MJ, and Timmerman H (1995) Molecular pharmacological aspects of histamine receptors. *Pharmacol Ther* **66**:413–463.

Liu C, Ma X, Jiang X, Wilson SJ, Hofstra CL, Blevitt J, Pyati J, Li X, Chai W, and Carruthers N et al. (2001) Cloning and pharmacological characterization of a fourth histamine receptor (H(4)) expressed in bone marrow. *Mol Pharmacol* **59**: 420–426.

Lohse MJ, Nikolaev VO, Hein P, Hoffmann C, Vilardaga J-P, and Bünemann M (2008) Optical techniques to analyze real-time activation and signaling of G-protein-coupled receptors. *Trends Pharmacol Sci* **29**:159–165.

Lohse MJ, Nuber S, and Hoffmann C (2012) Fluorescence/bioluminescence resonance energy transfer techniques to study G-protein-coupled receptor activation and signaling. *Pharmacol Rev* **64**:299–336.

Lutz S, Shankaranarayanan A, Coco C, Ridilla M, Nance MR, Vettel C, Baltus D, Evelyn CR, Neubig RR, and Wieland T et al. (2007) Structure of Galphaq-p63RhoGEF-RhoA complex reveals a pathway for the activation of RhoA by GPCRs. *Science* **318**:1923–1927.

Martins SAM, Trabuco JRC, Monteiro GA, Chu V, Conde JP, and Prazeres DMF (2012) Towards the miniaturization of GPCR-based live-cell screening assays. *Trends Biotechnol* **30**:566–574.

Marullo S and Bouvier M (2007) Resonance energy transfer approaches in molecular pharmacology and beyond. *Trends Pharmacol Sci* **28**:362–365.

Medina VA and Rivera ES (2010) Histamine receptors and cancer pharmacology. *Br J Pharmacol* **161**:755–767.

Murayama T, Kajiyama Y, and Nomura Y (1990) Histamine-stimulated and GTP-binding proteins-mediated phospholipase A2 activation in rabbit platelets. *J Biol Chem* **265**:4290–4295.

Nagai T, Yamada S, Tominaga T, Ichikawa M, and Miyawaki A (2004) Expanded dynamic range of fluorescent indicators for Ca(2+) by circularly permuted yellow fluorescent proteins. *Proc Natl Acad Sci USA* **101**:10554–10559.

Ostermaier MK, Schertler GF, and Standfuss J (2014) Molecular mechanism of phosphorylation-dependent arrestin activation. *Curr Opin Struct Biol* **29**:143–151.

Parsons ME and Ganellin CR (2006) Histamine and its receptors. *Br J Pharmacol* **147** (Suppl 1):S127–S135.

Piljić A and Schultz C (2008) Simultaneous recording of multiple cellular events by FRET. *ACS Chem Biol* **3**:156–160.
Pino-Ángeles A, Reyes-Palomares A, Melgarejo E, and Sánchez-Jiménez F (2012) Histamine: an undercover agent in multiple rare diseases? *J Cell Mol Med* **16**:1947–1960.
Sackmann EK, Fulton AL, and Beebe DJ (2014) The present and future role of microfluidics in biomedical research. *Nature* **507**:181–189.
Schrage R, Schmitz A-L, Gaffal E, Annala S, Kehraus S, Wenzel D, Büllesbach KM, Bald T, Inoue A, and Shinjo Y et al. (2015) The experimental power of FR900359 to study Gq-regulated biological processes. *Nat Commun* **6**:10156.
Schröder R, Janssen N, Schmidt J, Kebig A, Merten N, Hennen S, Müller A, Blättermann S, Mohr-Andrä M, and Zahn S et al. (2010) Deconvolution of complex G protein-coupled receptor signaling in live cells using dynamic mass redistribution measurements. *Nat Biotechnol* **28**:943–949.
Seifert R, Grünbaum L, and Schultz G (1994) Histamine H1-receptors in HL-60 monocytes are coupled to Gi-proteins and pertussis toxin-insensitive G-proteins and mediate activation of Ca2+ influx without concomitant Ca2+ mobilization from intracellular stores. *Naunyn Schmiedebergs Arch Pharmacol* **349**: 355–361.
Seifert R, Strasser A, Schneider EH, Neumann D, Dove S, and Buschauer A (2013) Molecular and cellular analysis of human histamine receptor subtypes. *Trends Pharmacol Sci* **34**:33–58.
Sensken S-C, Stäubert C, Keul P, Levkau B, Schöneberg T, and Gräler MH (2008) Selective activation of G alpha i mediated signalling of S1P3 by FTY720-phosphate. *Cell Signal* **20**:1125–1133.
Smrcka AV (2008) G protein βγ subunits: central mediators of G protein-coupled receptor signaling. *Cell Mol Life Sci* **65**:2191–2214.
Stoddart LA, White CW, Nguyen K, Hill SJ, and Pfleger KDG (2015) Fluorescence- and bioluminescence-based approaches to study GPCR ligand binding. *Br J Pharmacol* DOI: 10.1111/bph.13316 [published ahead of print].
Stumpf AD and Hoffmann C (2016) Optical probes based on G protein-coupled receptors - added work or added value? *Br J Pharmacol* **173**:255–266.
Thomsen W, Frazer J, and Unett D (2005) Functional assays for screening GPCR targets. *Curr Opin Biotechnol* **16**:655–665.
Thurmond RL, Gelfand EW, and Dunford PJ (2008) The role of histamine H1 and H4 receptors in allergic inflammation: the search for new antihistamines. *Nat Rev Drug Discov* **7**:41–53.
Tsvetanova NG, Irannejad R, and von Zastrow M (2015) G protein-coupled receptor (GPCR) signaling via heterotrimeric G proteins from endosomes. *J Biol Chem* **290**: 6689–6696.
van Rijssel J and van Buul JD (2012) The many faces of the guanine-nucleotide exchange factor trio. *Cell Adhes Migr* **6**:482–487.
van Unen J, Reinhard NR, Yin T, Wu YI, Postma M, Gadella TWJ, and Goedhart J (2015a) Plasma membrane restricted RhoGEF activity is sufficient for RhoA-mediated actin polymerization. *Sci Rep* **5**:14693.
van Unen J, Stumpf AD, Schmid B, Reinhard NR, Hordijk PL, Hoffmann C, Gadella TWJ, Jr, and Goedhart J (2016) A New Generation of FRET Sensors for Robust Measurement of Gαi1, Gαi2 and Gαi3 Activation Kinetics in Single Cells. *PLoS One* **11**:e0146789.
van Unen J, Woolard J, Rinken A, Hoffmann C, Hill S, Goedhart J, Bruchas M, Bouvier M, and Adjobo-Hermans M (2015b) A Perspective on Studying G-Protein-Coupled Receptor Signaling with Resonance Energy Transfer Biosensors in Living Organisms. *Mol Pharmacol* **88**:589–595.
Verbeek DS, Goedhart J, Bruinsma L, Sinke RJ, and Reits EA (2008) PKC gamma mutations in spinocerebellar ataxia type 14 affect C1 domain accessibility and kinase activity leading to aberrant MAPK signaling. *J Cell Sci* **121**:2339–2349.
Vilardaga J-P, Bünemann M, Krasel C, Castro M, and Lohse MJ (2003) Measurement of the millisecond activation switch of G protein-coupled receptors in living cells. *Nat Biotechnol* **21**:807–812.
Vilardaga J-P, Jean-Alphonse FG, and Gardella TJ (2014) Endosomal generation of cAMP in GPCR signaling. *Nat Chem Biol* **10**:700–706.
Zhu X, Jiang M, and Birnbaumer L (1998) Receptor-activated Ca2+ influx via human Trp3 stably expressed in human embryonic kidney (HEK)293 cells. Evidence for a non-capacitative Ca2+ entry. *J Biol Chem* **273**:133–142.
Zhu Y, Michalovich D, Wu H, Tan KB, Dytko GM, Mannan IJ, Boyce R, Alston J, Tierney LA, and Li X et al. (2001) Cloning, expression, and pharmacological characterization of a novel human histamine receptor. *Mol Pharmacol* **59**:434–441.

Address correspondence to: Joachim Goedhart, University of Amsterdam, P.O. Box 94215, NL-1090 GE Amsterdam, The Netherlands. E-mail: j.goedhart@uva.nl

Supplementary information

Quantitative single cell analysis of signaling pathways activated immediately downstream of histamine receptor subtypes

Jakobus van Unen, Ali Rashidfarrokhi, Eelco Hoogendoorn, Marten Postma, Theodorus W.J. Gadella Jr., Joachim Goedhart

Molecular Pharmacology

Supplemental Figure 1

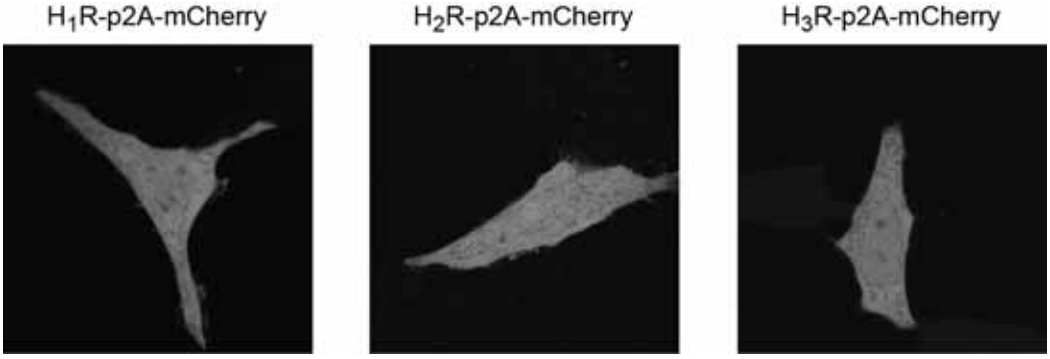

Representative images of the mCherry fluorescence in HeLa cells transfected with either Histamine-1, Histamine-2 or Histamine-3 receptors fused to p2A-mCherry. Width of the individual images corresponds to 73µm.

Supplemental Figure 2

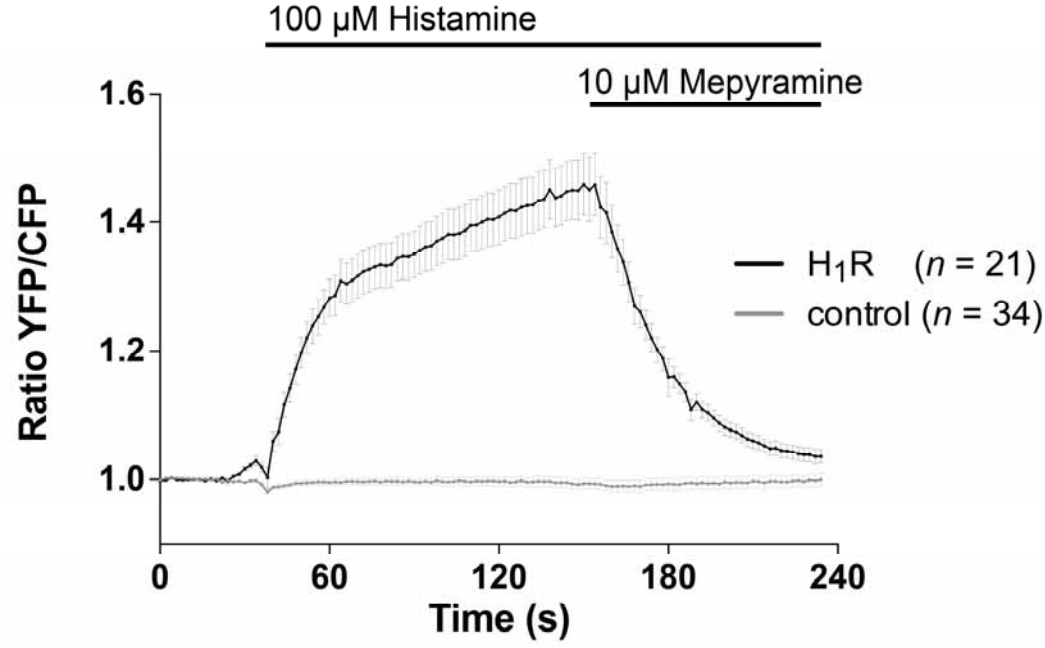

HEK293 cells transfected with H_1R-p2A-RFP and the DORA RhoA biosensor show a fast and reversible change in YFP/CFP ratio upon stimulation with histamine and mepyramine (*black*). Control cells transfected with the DORA RhoA biosensor do not show any change in YFP/CFP ratio upon stimulation with histamine and mepyramine (*grey*). HEK293 cells were stimulated with histamine at t = 32s and the response was antagonized by the addition of mepyramine at t = 152s. Time traces show the average ratio change of YFP/CFP fluorescence (± s.e.m).

Supplemental Figure 3

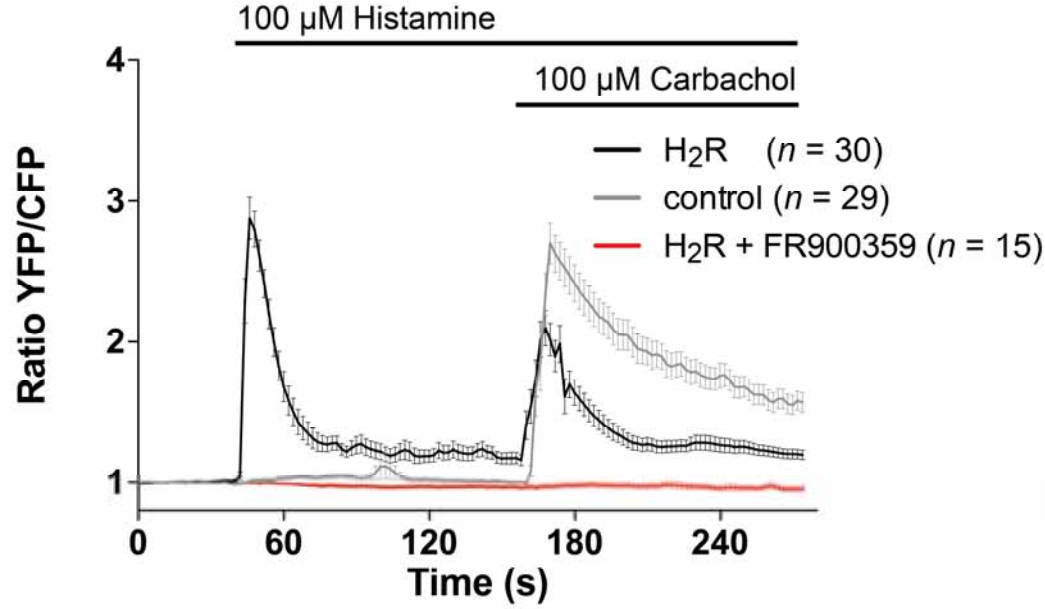

HEK293 cells transfected with H_2R-p2A-RFP and the Ycam biosensor show a fast transient change in YFP/CFP ratio upon stimulation with histamine and a slightly sustained increased ratio. Subsequent stimulation with Carbachol shows another fast transient change in the YFP/CFP ratio, resulting in a sustained elevated ratio (*black*). Control cells transfected with the Ycam biosensor do not show any change in YFP/CFP ratio upon stimulation with histamine and show a fast change in YFP/CFP ratio upon stimulation with carbachol (*grey*). Cells treated for 1 hour with the Gαq inhibitor FR900359, and transfected with H_2R-p2A-RFP and the Ycam biosensor do not show any change in YFP/CFP ratio upon stimulation with histamine or carbachol. HEK293 cells were stimulated with histamine at t = 40s and stimulated with carbachol at t = 160s. Time traces show the average ratio change of YFP/CFP fluorescence (± s.e.m).

Supplemental Figure 4

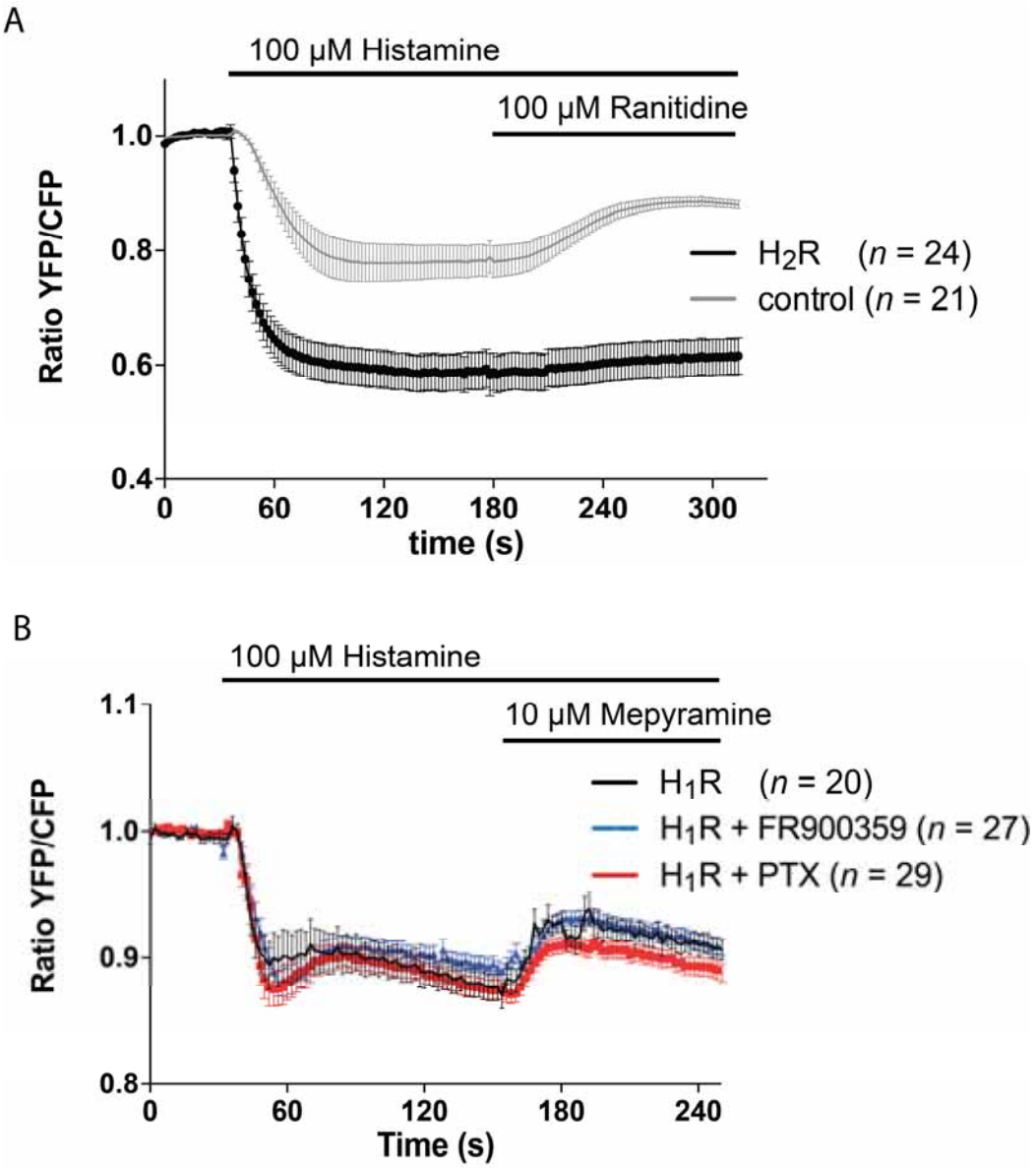

(A) HEK293 cells transfected with H_2R-p2A-RFP and the $^{T}EPAC^{VV}$ biosensor show a fast change in YFP/CFP ratio upon stimulation with histamine and a minimal recovery after addition of ranitidine (*black*). Control cells transfected with the $^{T}EPAC^{VV}$ biosensor show a fast change in YFP/CFP ratio upon stimulation with histamine and partial recovery after addition of ranitidine (*grey*). (B) Hela cells transfected with H_1R-p2A-RFP and the $^{T}EPAC^{VV}$ biosensor show a small fast and reversible change in YFP/CFP ratio upon stimulation with histamine and mepyramine (*black*). Hela cells transfected with

H_1R-p2A-RFP and the ^{T}EPAC^{VV} biosensor, and treated overnight with 100ng/ml Pertussis Toxin (PTX) or treated for 2 hours with 2μM of a Gαq inhibitor FR900359, also show a small fast and reversible change in YFP/CFP ratio upon stimulation with histamine and mepyramine (*red and blue, respectively*). HEK293 (A)/HeLa (B) cells were stimulated with histamine at *t* = 32s and the response was antagonized by the addition of ranitidine (A) at *t* = 172s or mepyramine (B) at *t* = 152s. Time traces show the average ratio change of YFP/CFP fluorescence (± s.e.m).

Supplemental Figure 5

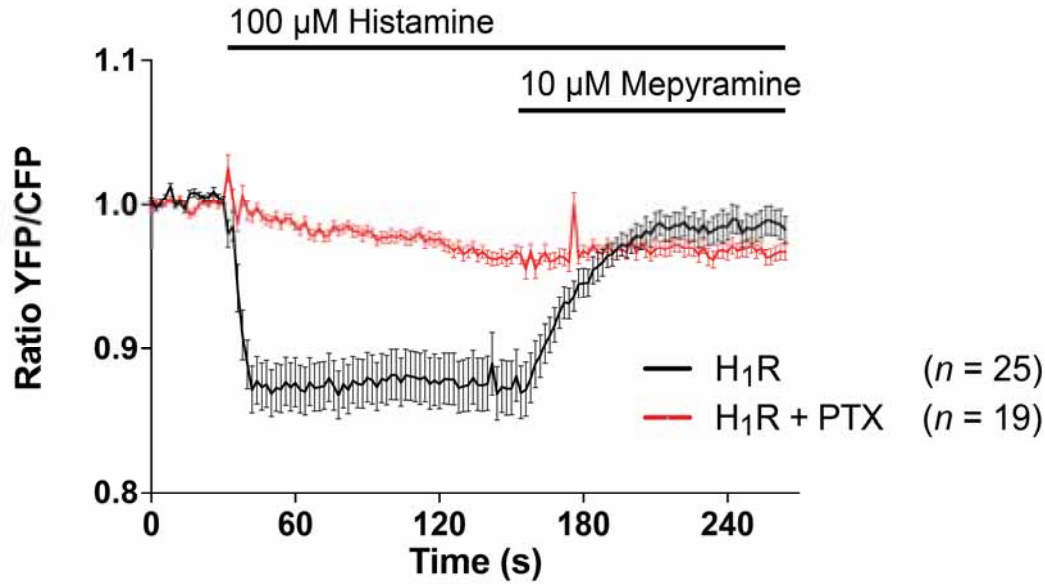

Hela cells transfected with H_1R-p2A-RFP and the Gαi biosensor show a fast and reversible change in YFP/CFP ratio upon stimulation with histamine and mepyramine (*black*). Cells treated overnight with 100ng/ml Pertussis Toxin (PTX), and transfected with H_1R-p2A-RFP and the Gαi biosensor do not show any change in YFP/CFP ratio upon stimulation with histamine and mepyramine (*red*). HeLA cells were stimulated with histamine at *t* = 32s and stimulated with mepyramine at *t* = 152s. Time traces show the average ratio change of YFP/CFP fluorescence (± s.e.m).

Supplemental Figure 6

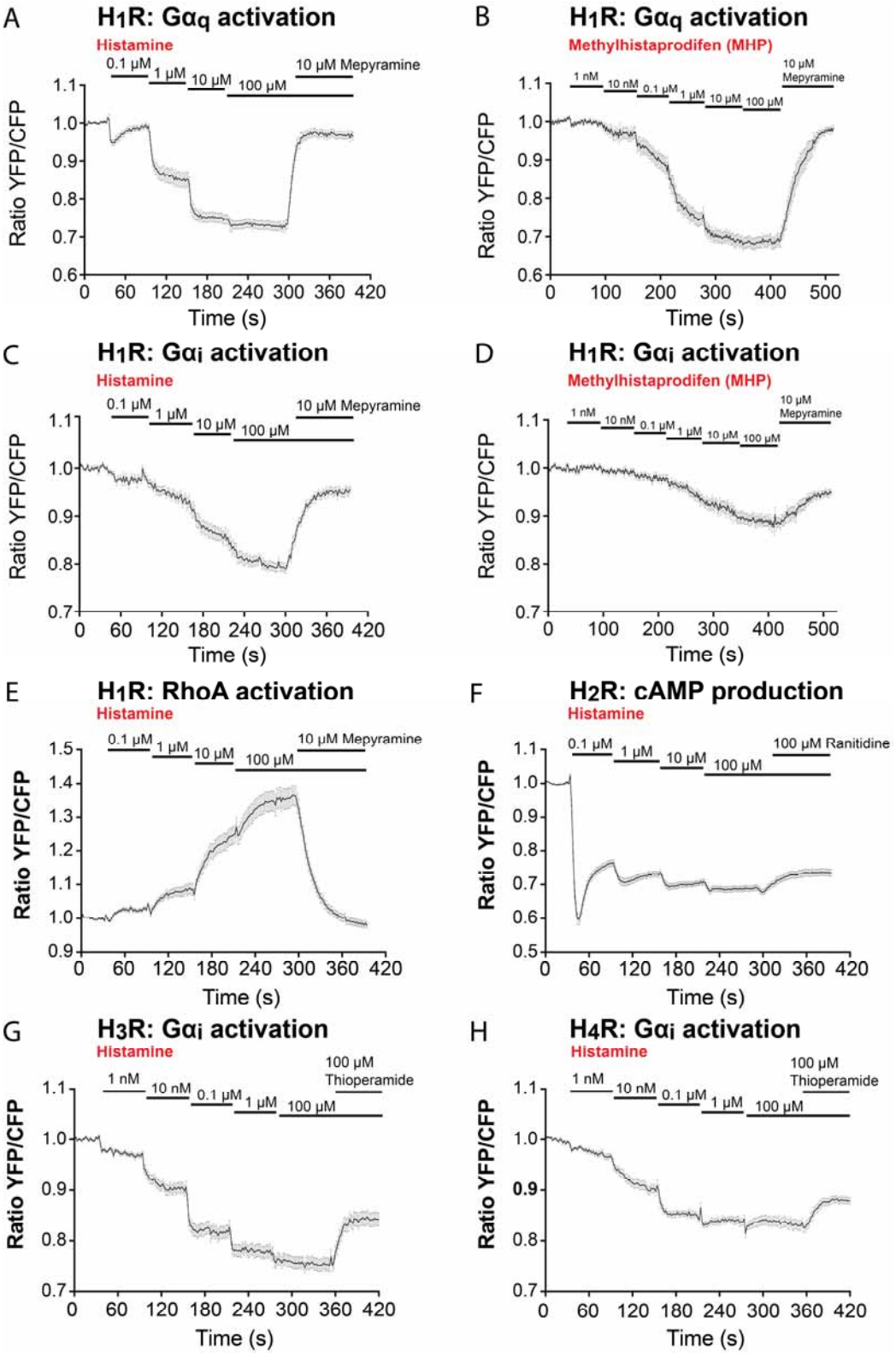

Single cell pharmacology measurements of the four histamine receptor isoforms. (A) Hela cells transfected with H_1R-p2A-RFP and the Gαq biosensor were stimulated with the indicated cumulative concentrations of histamine at *t* = 32s, *t* = 92, *t* = 152, *t* = 212, and subsequently antagonized with mepyramine at *t* = 292 (*n* = 26). (B) Hela cells transfected with H_1R-p2A-RFP and the Gαq biosensor were stimulated with the indicated cumulative concentrations of methylhistaprodifen at *t* = 32s, *t* = 92, *t* = 152, *t* = 212, *t* = 272, *t* = 332 and subsequently antagonized with mepyramine at *t* = 412 (*n* = 17). (C) Hela cells transfected with H_1R-p2A-RFP and the Gαi biosensor were stimulated with the indicated cumulative concentrations of histamine at *t* = 32s, *t* = 92, *t* = 152, *t* = 212, and subsequently antagonized with mepyramine at *t* = 292 (*n* = 17). (D) Hela cells transfected with H_1R-p2A-RFP and the Gαi biosensor were stimulated with the indicated cumulative concentrations of methylhistaprodifen at *t* = 32s, *t* = 92, *t* = 152, *t* = 212, *t* = 272, *t* = 332 and subsequently antagonized with mepyramine at *t* = 412 (*n* = 10). (E) Hela cells transfected with H_1R-p2A-RFP and the DORA RhoA biosensor were stimulated with the indicated cumulative concentrations of histamine at *t* = 32s, *t* = 92, *t* = 152, *t* = 212, and subsequently antagonized with mepyramine at *t* = 292 (*n* = 44). (F) Hela cells transfected with H_2R-p2A-RFP and the ^{T}EPAC^{VV} biosensor were stimulated with the indicated cumulative concentrations of histamine at *t* = 32s, *t* = 92, *t* = 152, *t* = 212, and subsequently antagonized with ranitidine at *t* = 292 (*n* = 32). (G) Hela cells transfected with H_3R-p2A-RFP and the Gαi biosensor were stimulated with the indicated cumulative concentrations of histamine at *t* = 32s, *t* = 92, *t* = 152, *t* = 212, *t* = 272 and subsequently antagonized with thioperamide at *t* = 292 (*n* = 29). (H) Hela cells transfected with H_4R-p2A-RFP and the Gαi biosensor were stimulated with the indicated cumulative concentrations of histamine at *t* = 32s, *t* = 92, *t* = 152, *t* = 212, *t* = 272 and subsequently antagonized with thioperamide at *t* = 292 (*n* = 16). Time traces show the average ratio change of YFP/CFP fluorescence (± s.e.m).